NASA TECHNICAL NOTE

NASA TN D-6296

NASA TN D-6296

DYNAMIC RECONSTRUCTION ERRORS IN DIGITAL-TO-ANALOG SYSTEMS WITH BIOMEDICAL APPLICATIONS

by William P. Dotson, Jr.

Manned Spacecraft Center
Houston, Texas 77058

NATIONAL AERONAUTICS AND SPACE ADMINISTRATION • WASHINGTON, D. C. • APRIL 1971

1. Report No.	2. Government Accession No.	3. Recipient's Catalog No.
NASA TN D-6296		

4. Title and Subtitle	5. Report Date
DYNAMIC RECONSTRUCTION ERRORS IN DIGITAL-TO-ANALOG SYSTEMS WITH BIOMEDICAL APPLICATIONS	April 1971
	6. Performing Organization Code

7. Author(s)	8. Performing Organization Report No.
William P. Dotson, Jr., MSC	MSC S-254
	10. Work Unit No.
	039-00-00-00-72

9. Performing Organization Name and Address	11. Contract or Grant No.
Manned Spacecraft Center Houston, Texas 77058	
	13. Type of Report and Period Covered
	Technical Note

12. Sponsoring Agency Name and Address	14. Sponsoring Agency Code
National Aeronautics and Space Administration Washington, D.C. 20546	

15. Supplementary Notes

16. Abstract

Various digital-to-analog conversion techniques are analyzed in order to determine their instantaneous error performance. The analytical technique is curve fitting of polynomials of zero to third order to the given digital sample points. Experimental results are also given on digitized electrocardiogram data processed through a third-order polynomial curve-fitting routine. This report demonstrates that a trade-off of system complexity (order of the polynomial) and transmission bandwidth is possible, with no decrease in the quality of the reconstructed data.

17. Key Words (Suggested by Author(s))	18. Distribution Statement
* Digital-to-Analog Converters * Digital-to-Analog Conversion Errors * Minimum Bandwidth Systems * Interpolation * Telemetry Systems	Unclassified — Unlimited

19. Security Classif. (of this report)	20. Security Classif. (of this page)	21. No. of Pages	22. Price*
None	None	43	$3.00

*For sale by the National Technical Information Service, Springfield, Virginia 22151

DYNAMIC RECONSTRUCTION ERRORS IN DIGITAL-TO-ANALOG SYSTEMS WITH BIOMEDICAL APPLICATIONS

By William P. Dotson, Jr.
Manned Spacecraft Center

SUMMARY

Available documentation on telemetry systems used to handle analog parameters from the Apollo spacecraft indicates that digital sampling rates of approximately $5f_c$ to $10f_c$ are used. (The term f_c is considered to be the highest frequency of interest in the spectrum of the analog signal.) The digital samples are then transmitted to a sample-and-hold digital-to-analog converter where the analog signal is reconstructed. This report presents an analysis of the worst-case dynamic errors of this reconstruction process and also the reconstruction processes up through the third order. The conclusion of this paper — based on experimental, as well as theoretical, results — is that certain classes of analog signals (for example, electrocardiogram signals) may have their sample rates reduced by a factor of 2 or more, while simultaneously the accuracy of the reconstructed signal is increased. This increase in accuracy is accomplished by using higher order reconstruction processes.

Reducing the sample rate of a parameter by a certain factor reduces the bandwidth requirement for that parameter by the same factor. Such a reduction in the bandwidth requirement would result in a significant easing of the present bandwidth problems between the remote sites and the Mission Control Center at the NASA Manned Spacecraft Center. Such benefits of a reduction in the sample rate (for example, easing bandwidth problems) are obvious. Other benefits would result from increasing the power spectral density of a radio-frequency down link (by decreasing the bandwidth), without increasing the spacecraft's transmitter power. This increase in the power spectral density should prove of particular benefit for lunar and deep-space probes where the down-link signal margins are seriously low. In situations where bandwidth is not a serious constraint, the sample rate could remain at its present level, and the accuracy of the reconstructed data could be significantly improved by going to high-order reconstruction processes.

INTRODUCTION

This study arose in connection with a problem concerning electrocardiograms. Briefly, the problem involved satisfying the requirement to transmit an electrocardiogram (EKG) for each of three astronauts from the spacecraft to the Mission Control

Center at the NASA Manned Spacecraft Center in real time. The bandwidth necessary to fulfill this requirement is the product of three electrocardiograms, 200 samples/sec/EKG, and 8 bits/sample, which gives 4800 bits/sec.

Additional bits must be added to this requirement of 4800 bits/sec for overhead in the telemetry formats. Furthermore, it would be most desirable to be able to satisfy other telemetry requirements at the same time, thereby adding still more to the required bandwidth.

The essence of the problem is that a bandwidth considerably in excess of 4800 bits/sec is needed to satisfy the bandwidth requirement if the present system concepts are used. Unfortunately, however, the available bandwidth from a remote site to the Goddard Space Flight Center is limited to 4800 bits/sec, including overhead in the telemetry formats.

It is clear, then, that the present system concepts must be changed to satisfy the basic requirement of transmitting three electrocardiograms in real time. Two approaches are immediately obvious:

1. Truncate each sample from an 8-bit to a 6-bit representation. This truncation will reduce the EKG bandwidth requirement to 3600 bits/sec at the expense of an increase in quantization noise.

2. Use a redundancy removal scheme (such as a zero-order predictor). Use of such a scheme may or may not reduce the bandwidth requirement, depending on the activity of the data; and implementation of such a scheme is fairly complex.

A third possible approach to the situation exists. If the sample rate is cut in half, the EKG bandwidth requirement drops to 2400 bits/sec. This sample-rate reduction would be simple to implement (by omitting every other sample), but would result in a decrease in the accuracy of the reconstructed signal if a zero-order reconstruction process were used. However, analysis of the error performance of different-order reconstruction processes shows that the error performance of a third-order digital-to-analog converter (DAC) at 100 samples/sec is better than that of a zero-order DAC at 200 samples/sec for any spectrum component less than 20 hertz. Most of the energy in an EKG spectrum lies below 20 hertz, and the fastest part of the analog waveform (the R-segment) exhibits a fundamental frequency of approximately 17 hertz.

The author would like to acknowledge the assistance of F. J. Wancho, who wrote the computer programs used in this study.

SYMBOLS

A	amplitude
B, C, D, E	coefficients of polynomial terms
f	frequency, Hz

f_c	cut-off frequency, Hz
f_s	sampling frequency, samples/sec
$\|G(f)\|$	root-mean-square spectrum of $g(t)$
$g(t)$	time function
m	ratio of the spectrum cut-off rate of the signal to 6 dB/octave
p	normalized sample rate, samples/cycle (or f_s/f)
T	period, 1/f, sec
t	time, sec
$y(t)$	time function
ϵ	error, percent or pulse-code-modulation (PCM) counts
ϵ_b	instantaneous error measured near the base-line crossing, percent
ϵ_p	instantaneous error measured at the peaks, percent
τ	sample period, sec
ω	radian frequency, $2\pi f$, rad/sec

NYQUIST SAMPLING THEOREM

The Nyquist sampling theorem states that if the root-mean-square spectrum $|G(f)|$ of the time function $g(t)$ is identically zero at all frequencies greater than f_c, then $g(t)$ is uniquely determined if its ordinates at a series of points spaced $1/(2f_c)$ seconds apart are known, with the series extending throughout the time domain (ref. 1). The theorem, as stated, does not consider two problems that always occur in the real world. The two problems are related to the following two statements.

1. Ideal band-limited signals do not exist.

2. Even if an ideal band-limited signal did exist, it would be necessary to pass its sampled values through an ideal low-pass filter with a cut-off frequency of $f_s/2$ in order to reconstruct exactly the analog signal.

Downing (ref. 1) has shown that the real-world signal may be considered to be band limited at the negative 3-decibel frequency for system design purposes, provided the following factors are known:

1. The rate of spectrum cut-off of the analog signal

2. The acceptable root-mean-square aliasing error

Knowledge of these factors permits a choice of the minimum sample rate to the negative 3-decibel frequency ratio. In the curves shown in figure 1 (ref. 1), m is the ratio of the spectrum cut-off rate of the signal to 6 dB/octave. It should be noted in using the curves shown in figure 1 that they presuppose the use of an ideal low-pass filter with a cut-off frequency of $f_s/2$ for the digital-to-analog conversion process. It should also be noted that the curves in figure 1 give the root-mean-square error and not the instantaneous error at any particular point on the analog waveform. The instantaneous error may be of considerable importance in the analysis of particular classes of data and is, in general, much greater than the root-mean-square error.

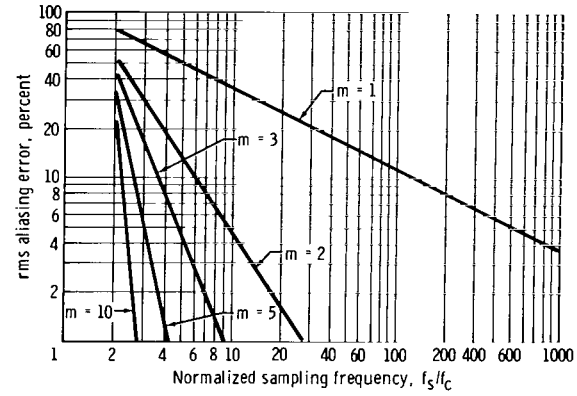

Figure 1. - Root-mean-square aliasing error as a function of normalized sampling frequency.

Ideal or optimum filtering for digital-to-analog conversion (or high-order reconstruction processes) minimizes both the root-mean-square and the instantaneous errors. Some remarks on optimum filtering for digital-to-analog conversion may be found in reference 1. This report is concerned with the instantaneous errors of digital-to-analog conversion processes by which a curve described by a polynomial in t is fitted to the given sample values.

DYNAMIC-RECONSTRUCTION ERRORS

The instantaneous error as a function of time between any two arbitrarily placed sample points is both difficult to find and difficult to use. Accordingly, in this section, the instantaneous errors will be found in two regions of interest. These regions are (1) near the base-line crossing of the analog signal and (2) at the peak of the analog signal. The time ordinates of the given samples have been selected so that both a meaningful result and a straightforward analysis can be obtained. Different choices in the placement of the sample points will, of course, result in different error equations, which, in most instances, will result in lower errors. The implication is that the analysis given is of a worst-case nature; and if random starting points for the sample locations were assumed, an average error, over many cycles, of approximately half the value of the worst-case errors could be expected.

Zero-Order DAC

Figure 2 is used to find the instantaneous error midway between two sample points for a zero-order DAC. This error is near the base-line crossing. The instantaneous error at $t = \tau/2$ for the sample-point locations shown in figure 2 is

$$\epsilon_b = \left| \frac{y\left(\frac{\tau}{2}\right) - y'\left(\frac{\tau}{2}\right)}{y_{max}} \right| (100) \qquad (1a)$$

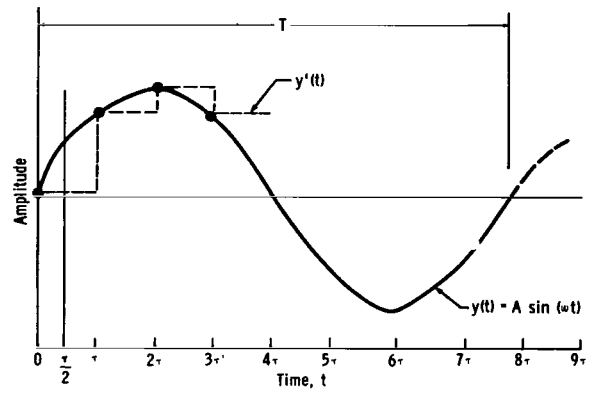

Figure 2. - Geometry for calculating ϵ_b for a zero-order DAC.

$$y(t) = A \sin(\omega t) \qquad (1b)$$

$$y'(t) = A \sin[\omega(0)] \qquad 0 \le t < \tau \qquad (1c)$$

$$y\left(\frac{\tau}{2}\right) = A \sin\left(\omega \frac{\tau}{2}\right) \qquad (1d)$$

$$y'\left(\frac{\tau}{2}\right) = 0 \qquad (1e)$$

$$y_{max} = A \qquad (1f)$$

$$\epsilon_b = 100 \sin\left(\omega \frac{\tau}{2}\right) \qquad \omega = \frac{2\pi}{T}$$

$$\tau = \frac{T}{p} \qquad (1g)$$

where p = normalized sample rate in samples/cycle

$$\epsilon_b = 100 \sin \frac{\pi}{p} \qquad (2)$$

Figure 3 is used to find the instantaneous error at the peaks for a zero-order DAC. The instantaneous error at t = 0 for the sample-point locations shown in figure 3 is

$$\epsilon_p = \left| \frac{y(0) - y'(0)}{y_{max}} \right| (100) \qquad (3a)$$

$$y(t) = A \sin \left[\omega \left(t + \frac{T}{4} \right) \right] \qquad (3b)$$

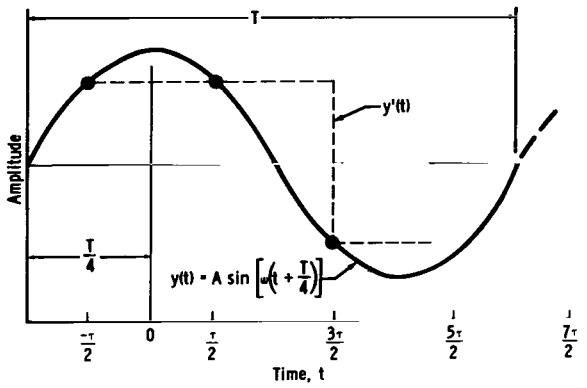

Figure 3. - Geometry for calculating ϵ_p for a zero-order DAC.

$$y'(t) = A \sin \left[\omega \left(-\frac{\tau}{2} + \frac{T}{4} \right) \right] \qquad -\frac{\tau}{2} \leq t < \frac{\tau}{2} \qquad (3c)$$

$$y(0) = A \sin \left[\omega \left(0 + \frac{T}{4} \right) \right] = A \qquad (3d)$$

$$y'(0) = A \sin \left[\omega \left(-\frac{\tau}{2} + \frac{T}{4} \right) \right] \qquad (3e)$$

$$y_{max} = A \qquad (3f)$$

$$\epsilon_p = 100 \left\{ 1 - \sin \left[\omega \left(-\frac{\tau}{2} + \frac{T}{4} \right) \right] \right\} \qquad \omega = \frac{2\pi}{T}$$

$$\tau = \frac{T}{p} \qquad (3g)$$

$$\epsilon_p = 100 \left\{ 1 - \sin \left[\pi \left(\frac{p - 2}{2p} \right) \right] \right\} \qquad (3h)$$

By using trigonometric identities, the equation

$$\epsilon_p = 100 \left(1 - \cos \frac{\pi}{p} \right) \qquad (4)$$

can be obtained. Equations (2) and (4) are plotted in figure 4.

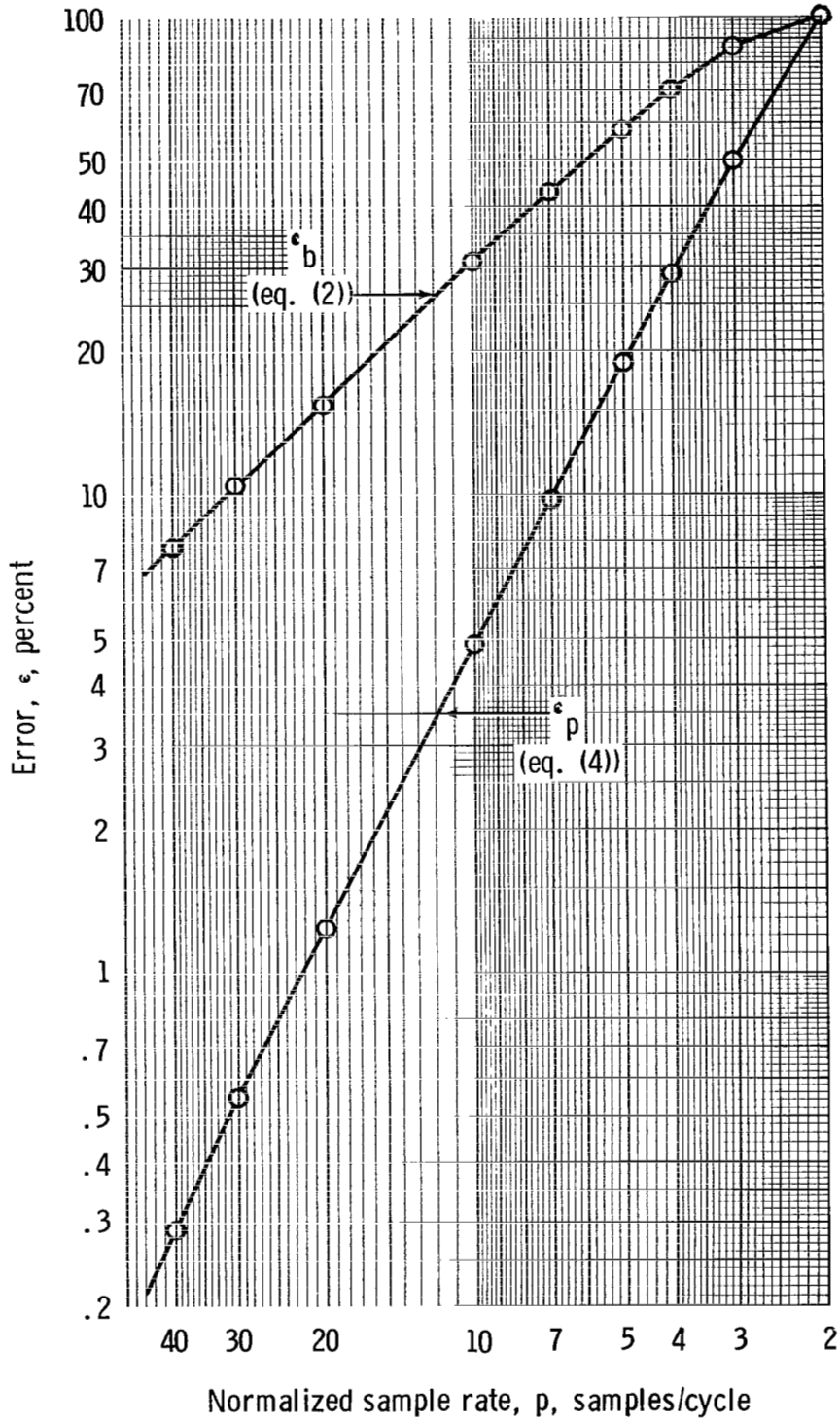

Figure 4. - Error as a function of normalized sample rate, zero-order DAC.

First-Order DAC

Figure 5 is used to find the instantaneous error midway between two sample points for a first-order DAC. This error is near the base-line crossing. The instantaneous error at $t = \tau/2$ for the sample-point locations shown in figure 5 is

$$\epsilon_b = \left| \frac{y\left(\frac{\tau}{2}\right) - y'\left(\frac{\tau}{2}\right)}{y_{max}} \right| (100) \qquad (5a)$$

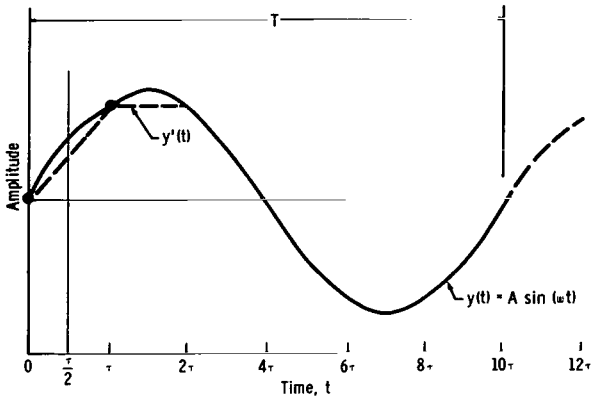

Figure 5. - Geometry for calculating ϵ_b for a first-order DAC.

$$y(t) = A \sin (\omega t) \qquad (5b)$$

$$y'(t) = 0 + \left[\frac{A \sin (\omega\tau)}{\tau}\right] t \qquad 0 \le t < \tau \qquad (5c)$$

$$y\left(\frac{\tau}{2}\right) = A \sin \left(\omega \frac{\tau}{2}\right) \qquad (5d)$$

$$y'\left(\frac{\tau}{2}\right) = \frac{1}{2} A \sin (\omega\tau) \qquad (5e)$$

$$y_{max} = A \qquad (5f)$$

$$\epsilon_b = 100\left[\sin \left(\omega \frac{\tau}{2}\right) - \frac{1}{2} \sin (\omega\tau)\right] \qquad \omega = \frac{2\pi}{T}$$

$$\tau = \frac{T}{p} \qquad (5g)$$

$$\epsilon_b = 100 \left(\sin \frac{\pi}{p} - \frac{1}{2} \sin \frac{2\pi}{p}\right) \qquad (6)$$

Figure 6 is used to find the instantaneous error at the peaks for a first-order DAC. The instantaneous error at $t = 0$ for the sample-point locations shown in figure 6 is

$$\epsilon_p = \left| \frac{y(0) - y'(0)}{y_{max}} \right| (100) \qquad (7a)$$

$$y(t) = A \sin \left[\omega \left(t + \frac{T}{4} \right) \right] \qquad (7b)$$

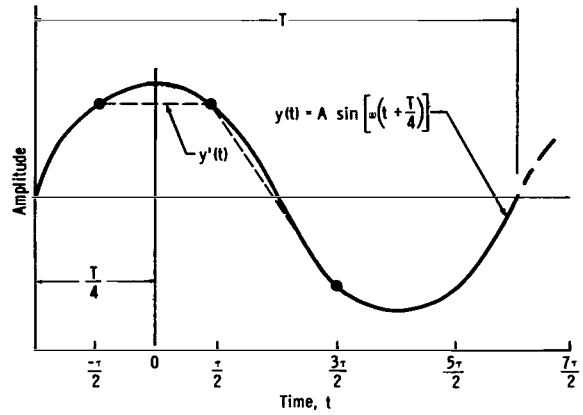

Figure 6. - Geometry for calculating ϵ_p for a first-order DAC.

$$y'(t) = A \sin \left[\omega \left(-\frac{\tau}{2} + \frac{T}{4} \right) \right] + \left\{ \frac{A \sin \left[\omega \left(\frac{\tau}{2} + \frac{T}{4} \right) \right] - A \sin \left[\omega \left(-\frac{\tau}{2} + \frac{T}{4} \right) \right]}{\tau} \right\} t \qquad -\frac{\tau}{2} \leq t < \frac{\tau}{2} \qquad (7c)$$

$$y(0) = A \sin \left(\omega \frac{T}{4} \right) = A \qquad (7d)$$

$$y'(0) = A \sin \left[\omega \left(-\frac{\tau}{2} + \frac{T}{4} \right) \right] \qquad (7e)$$

$$y_{max} = A \qquad (7f)$$

$$\epsilon_p = 100 \left\{ 1 - \sin \left[\omega \left(-\frac{\tau}{2} + \frac{T}{4} \right) \right] \right\} \qquad \omega = \frac{2\pi}{T}$$

$$\tau = \frac{T}{p} \qquad (7g)$$

$$\epsilon_p = 100 \left\{ 1 - \sin \left[\pi \left(\frac{p - 2}{2p} \right) \right] \right\} \qquad (7h)$$

By using trigonometric identities, the equation

$$\epsilon_p = 100\left(1 - \cos\frac{\pi}{p}\right) \tag{8}$$

can be obtained. Equations (6) and (8) are plotted in figure 7.

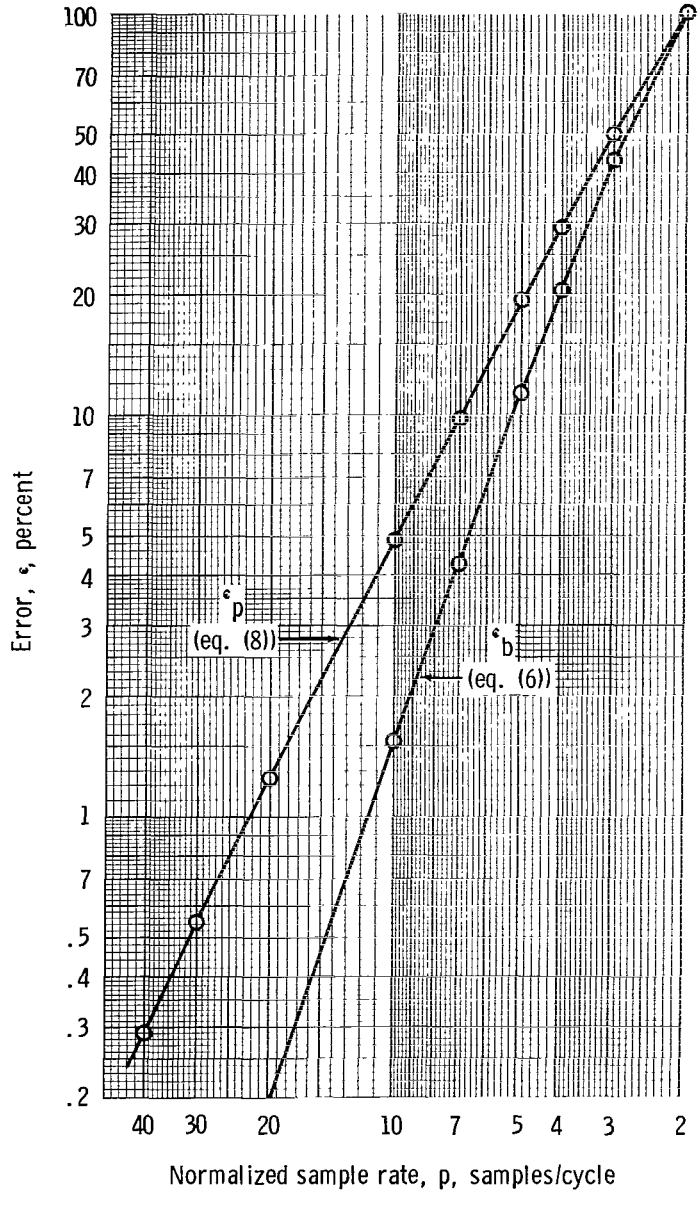

Figure 7. - Error as a function of normalized sample rate, first-order DAC.

Second-Order DAC

Figure 8 is used to find the instantaneous error midway between two sample points for a second-order DAC. This error is near the base-line crossing. The instantaneous error at $t = 0$ for the sample-point locations shown in figure 8 is

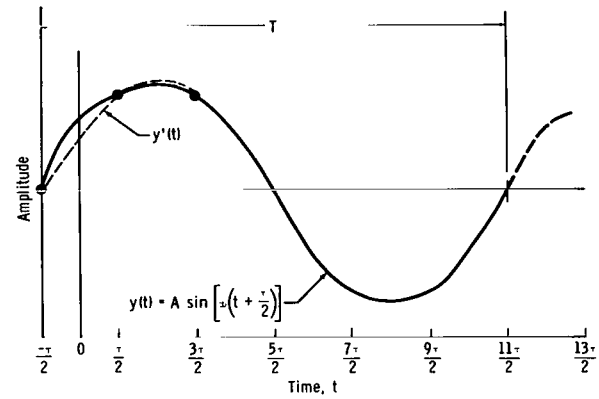

Figure 8. - Geometry for calculating ϵ_b for a second-order DAC.

$$\epsilon_b = \left| \frac{y(0) - y'(0)}{y_{max}} \right| (100) \qquad (9a)$$

$$y(t) = A \sin \left[\omega \left(t + \frac{\tau}{2} \right) \right] \qquad (9b)$$

$$y'(t) = Ct^2 + Dt + E \qquad -\frac{\tau}{2} \leq t < \frac{3\tau}{2} \qquad (9c)$$

$$y(0) = A \sin \left(\omega \frac{\tau}{2} \right) \qquad (9d)$$

$$y'(0) = E \qquad (9e)$$

$$y_{max} = A \qquad (9f)$$

$$\epsilon_b = 100 \left[\sin \left(\omega \frac{\tau}{2} \right) - \frac{E}{A} \right] \qquad (10)$$

To find E, solve the set

$$y'\left(-\frac{\tau}{2}\right) = C\left(-\frac{\tau}{2}\right)^2 + D\left(-\frac{\tau}{2}\right) + E = A \sin \left[\omega \left(-\frac{\tau}{2} + \frac{\tau}{2} \right) \right] = 0 \qquad (11a)$$

$$y'\left(\frac{\tau}{2}\right) = C\left(\frac{\tau}{2}\right)^2 + D\left(\frac{\tau}{2}\right) + E = A \sin (\omega\tau) \qquad (11b)$$

$$y'\left(\frac{3\tau}{2}\right) = C\left(\frac{3\tau}{2}\right)^2 + D\left(\frac{3\tau}{2}\right) + E = A \sin(2\omega\tau) \tag{11c}$$

$$E = -\frac{A}{8}\left[\sin(2\omega\tau) - 6\sin(\omega\tau)\right] \tag{11d}$$

$$\epsilon_b = 100\left\{\sin\left(\omega\frac{\tau}{2}\right) - \frac{1}{8}\left[6\sin(\omega\tau) - \sin(2\omega\tau)\right]\right\} \qquad \omega = \frac{2\pi}{T}$$

$$\tau = \frac{T}{p} \tag{11e}$$

$$\epsilon_b = 100\left[\sin\frac{\pi}{p} - \frac{1}{8}\left(6\sin\frac{2\pi}{p} - \sin\frac{4\pi}{p}\right)\right] \tag{12}$$

Figure 9 is used to find the instantaneous error at the peaks for a second-order DAC. The instantaneous error at $t = 0$ for the sample-point locations shown in figure 9 is

$$\epsilon_p = \left|\frac{y(0) - y'(0)}{y_{max}}\right|(100) \tag{13a}$$

$$y(t) = A \sin\left[\omega\left(t + \frac{T}{4}\right)\right] \tag{13b}$$

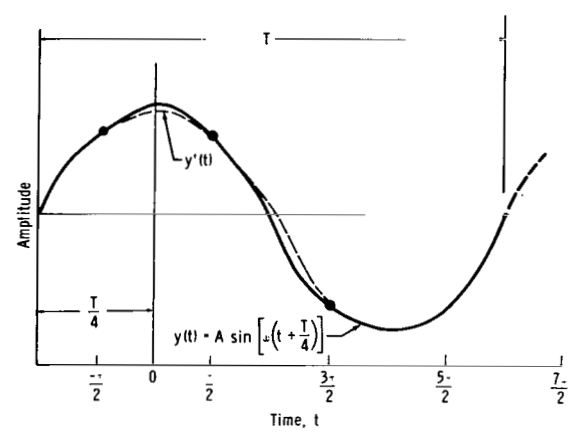

Figure 9. - Geometry for calculating ϵ_p for a second-order DAC.

$$y'(t) = Ct^2 + Dt + E \qquad -\frac{\tau}{2} \le t < \frac{3\tau}{2} \tag{13c}$$

$$y(0) = A \sin\left(\omega\frac{T}{4}\right) = A \tag{13d}$$

$$y'(0) = E \tag{13e}$$

$$y_{max} = A \tag{13f}$$

$$\epsilon_p = 100\left(1 - \frac{E}{A}\right) \tag{14}$$

To find E, solve the set

$$y'\left(-\frac{\tau}{2}\right) = C\left(-\frac{\tau}{2}\right)^2 + D\left(-\frac{\tau}{2}\right) + E = A \sin\left[\omega\left(-\frac{\tau}{2} + \frac{T}{4}\right)\right] \tag{15a}$$

$$y'\left(\frac{\tau}{2}\right) = C\left(\frac{\tau}{2}\right)^2 + D\left(\frac{\tau}{2}\right) + E = A \sin\left[\omega\left(\frac{\tau}{2} + \frac{T}{4}\right)\right] \tag{15b}$$

$$y'\left(\frac{3\tau}{2}\right) = C\left(\frac{3\tau}{2}\right)^2 + D\left(\frac{3\tau}{2}\right) + E = A \sin\left[\omega\left(\frac{3\tau}{2} + \frac{T}{4}\right)\right] \tag{15c}$$

$$E = \frac{A}{8}\left\{3 \sin\left[\omega\left(-\frac{\tau}{2} + \frac{T}{4}\right)\right] + 6 \sin\left[\omega\left(\frac{\tau}{2} + \frac{T}{4}\right)\right] - \sin\left[\omega\left(\frac{3\tau}{2} + \frac{T}{4}\right)\right]\right\} \qquad \omega = \frac{2\pi}{T}$$

$$\tau = \frac{T}{p} \tag{15d}$$

$$\epsilon_p = 100\left(1 - \frac{1}{8}\left\{6 \sin\left[\pi\left(\frac{p+2}{2p}\right)\right] + 3 \sin\left[\pi\left(\frac{p-2}{2p}\right)\right] - \sin\left[\pi\left(\frac{p+6}{2p}\right)\right]\right\}\right) \tag{15e}$$

By using trigonometric identities, the equation

$$\epsilon_p = 100\left[1 - \frac{1}{8}\left(9 \cos\frac{\pi}{p} - \cos\frac{\pi}{3p}\right)\right] \tag{16}$$

can be obtained. Equations (12) and (16) are plotted in figure 10.

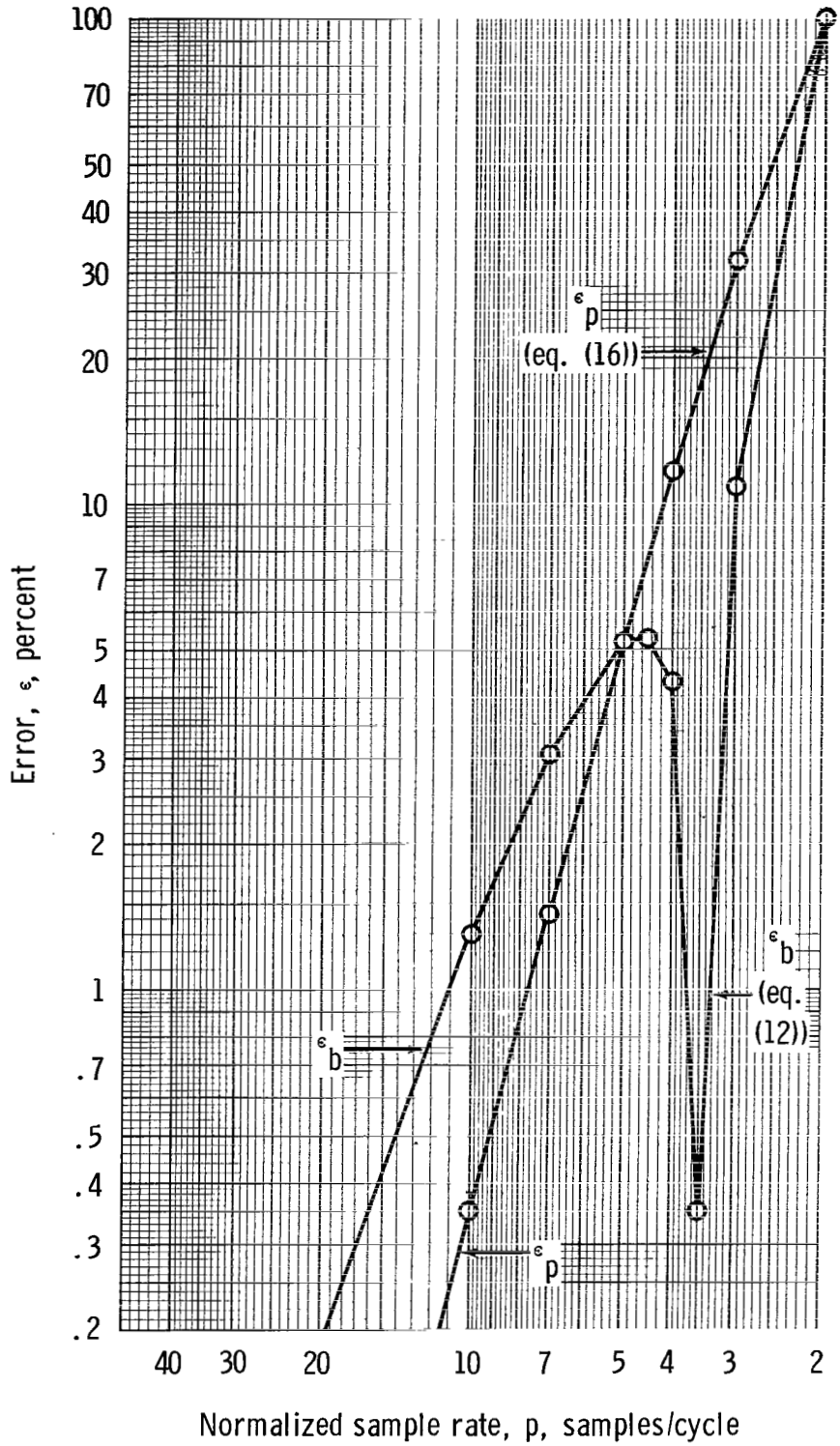

Figure 10. - Error as a function of normalized sample rate, second-order DAC.

Third-Order DAC

Figure 11 is used to find the instantaneous error midway between two sample points for a third-order DAC. This error is near the base-line crossing. The instantaneous error at $t = 0$ for the sample-point locations shown in figure 11 is

$$\epsilon_b = \left| \frac{y(0) - y'(0)}{y_{max}} \right| (100) \qquad (17a)$$

$$y(t) = A \sin \left[\omega \left(t + \frac{T}{2} + \frac{\tau}{2} \right) \right] \qquad (17b)$$

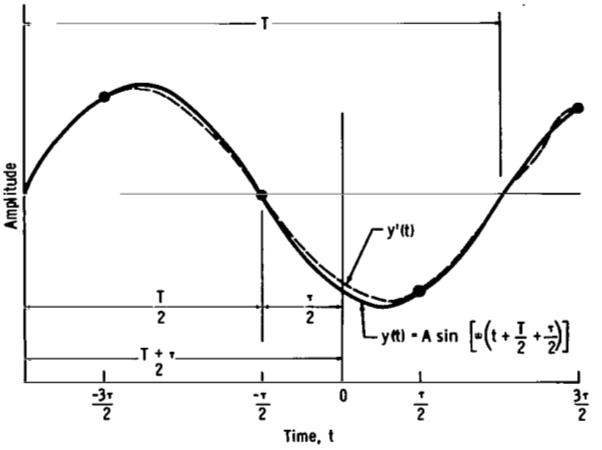

Figure 11. - Geometry for calculating ϵ_b for a third-order DAC.

$$y'(t) = Bt^3 + Ct^2 + Dt + E \qquad -\frac{3\tau}{2} \le t < \frac{3\tau}{2} \qquad (17c)$$

$$y(0) = A \sin \left[\omega \left(\frac{T}{2} + \frac{\tau}{2} \right) \right] \qquad (17d)$$

$$y'(0) = E \qquad (17e)$$

$$y_{max} = A \qquad (17f)$$

$$\epsilon_b = 100 \left\{ \sin \left[\omega \left(\frac{T}{2} + \frac{\tau}{2} \right) \right] - \frac{E}{A} \right\} \qquad (18)$$

To find E, solve the set

$$y'\left(-\frac{3\tau}{2}\right) = B\left(-\frac{3\tau}{2}\right)^3 + C\left(-\frac{3\tau}{2}\right)^2 + D\left(-\frac{3\tau}{2}\right) + E = A \sin \left[\omega \left(\frac{T}{2} - \tau \right) \right] \qquad (19a)$$

$$y'\left(-\frac{\tau}{2}\right) = B\left(-\frac{\tau}{2}\right)^3 + C\left(-\frac{\tau}{2}\right)^2 + D\left(-\frac{\tau}{2}\right) + E = A \sin \left(\omega \frac{T}{2} \right) = 0 \qquad (19b)$$

$$y'\left(\frac{\tau}{2}\right) = B\left(\frac{\tau}{2}\right)^3 + C\left(\frac{\tau}{2}\right)^2 + D\left(\frac{\tau}{2}\right) + E = A \sin\left[\omega\left(\frac{T}{2} + \tau\right)\right] \tag{19c}$$

$$y'\left(\frac{3\tau}{2}\right) = B\left(\frac{3\tau}{2}\right)^3 + C\left(\frac{3\tau}{2}\right)^2 + D\left(\frac{3\tau}{2}\right) + E = A \sin\left[\omega\left(\frac{T}{2} + 2\tau\right)\right] \tag{19d}$$

$$E = \frac{A}{16}\left\{9 \sin\left[\omega\left(\frac{T}{2} + \tau\right)\right] - \sin\left[\omega\left(\frac{T}{2} - \tau\right)\right] - \sin\left[\omega\left(\frac{T}{2} + 2\tau\right)\right]\right\} \tag{19e}$$

$$\epsilon_b = 100\left(\sin\left[\omega\left(\frac{T}{2} + \frac{\tau}{2}\right)\right] - \frac{1}{16}\left\{9 \sin\left[\omega\left(\frac{T}{2} + \tau\right)\right] - \sin\left[\omega\left(\frac{T}{2} - \tau\right)\right] - \sin\left[\omega\left(\frac{T}{2} + 2\tau\right)\right]\right\}\right) \qquad \omega = \frac{2\pi}{T} \qquad \tau = \frac{T}{p} \tag{19f}$$

$$\epsilon_b = 100\left(\sin\left[\pi\left(\frac{p+1}{p}\right)\right] - \frac{1}{16}\left\{9 \sin\left[\pi\left(\frac{p+2}{p}\right)\right] - \sin\left[\pi\left(\frac{p-2}{p}\right)\right] - \sin\left[\pi\left(\frac{p+4}{p}\right)\right]\right\}\right) \tag{19g}$$

By using trigonometric identities, the equation

$$\epsilon_b = 100\left[-\sin\frac{\pi}{p} + \frac{1}{16}\left(10 \sin\frac{2\pi}{p} - \sin\frac{4\pi}{p}\right)\right] \tag{20}$$

can be obtained.

Figure 12 is used to find the instantaneous error at the peaks for a third-order DAC. The instantaneous error at $t = 0$ for the sample-point locations shown in figure 12 is

$$\epsilon_p = \left|\frac{y(0) - y'(0)}{y_{max}}\right|(100) \tag{21a}$$

$$y(t) = A \sin\left[\omega\left(t + \frac{T}{4}\right)\right] \tag{21b}$$

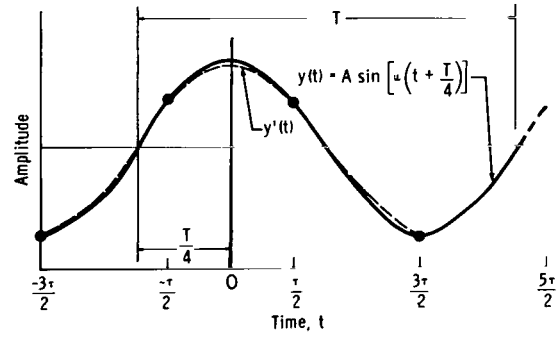

Figure 12. - Geometry for calculating ϵ_p for a third-order DAC.

$$y'(t) = Bt^3 + Ct^2 + Dt + E \qquad -\frac{3\tau}{2} \le t < \frac{3\tau}{2} \tag{21c}$$

$$y(0) = A \sin\left(\omega \frac{T}{4}\right) = A \tag{21d}$$

$$y'(0) = E \tag{21e}$$

$$y_{max} = A \tag{21f}$$

$$\epsilon_p = 100\left(1 - \frac{E}{A}\right) \tag{22}$$

To find E, solve the set

$$y'\left(-\frac{3\tau}{2}\right) = B\left(-\frac{3\tau}{2}\right)^3 + C\left(-\frac{3\tau}{2}\right)^2 + D\left(-\frac{3\tau}{2}\right) + E = A \sin\left[\omega\left(\frac{T}{4} - \frac{3\tau}{2}\right)\right] \tag{23a}$$

$$y'\left(-\frac{\tau}{2}\right) = B\left(-\frac{\tau}{2}\right)^3 + C\left(-\frac{\tau}{2}\right)^2 + D\left(-\frac{\tau}{2}\right) + E = A \sin\left[\omega\left(\frac{T}{4} - \frac{\tau}{2}\right)\right] \tag{23b}$$

$$y'\left(\frac{\tau}{2}\right) = B\left(\frac{\tau}{2}\right)^3 + C\left(\frac{\tau}{2}\right)^2 + D\left(\frac{\tau}{2}\right) + E = A \sin\left[\omega\left(\frac{T}{4} + \frac{\tau}{2}\right)\right] \tag{23c}$$

$$y'\left(\frac{3\tau}{2}\right) = B\left(\frac{3\tau}{2}\right)^3 + C\left(\frac{3\tau}{2}\right)^2 + D\left(\frac{3\tau}{2}\right) + E = A \sin\left[\omega\left(\frac{T}{4} + \frac{3\tau}{2}\right)\right] \tag{23d}$$

$$E = \frac{A}{16}\left(9\left\{\sin\left[\omega\left(\frac{T}{4} - \frac{\tau}{2}\right)\right] + \sin\left[\omega\left(\frac{T}{4} + \frac{\tau}{2}\right)\right]\right\} - \left\{\sin\left[\omega\left(\frac{T}{4} - \frac{3\tau}{2}\right)\right] + \sin\left[\omega\left(\frac{T}{4} + \frac{3\tau}{2}\right)\right]\right\}\right) \qquad \omega = \frac{2\pi}{T}$$

$$\tau = \frac{T}{p} \tag{23e}$$

By using trigonometric identities, the equation

$$\epsilon_p = 100\left[1 - \frac{1}{8}\left(9 \cos \frac{\pi}{p} - \cos \frac{3\pi}{p}\right)\right] \tag{24}$$

can be obtained. Equations (20) and (24) are plotted in figure 13.

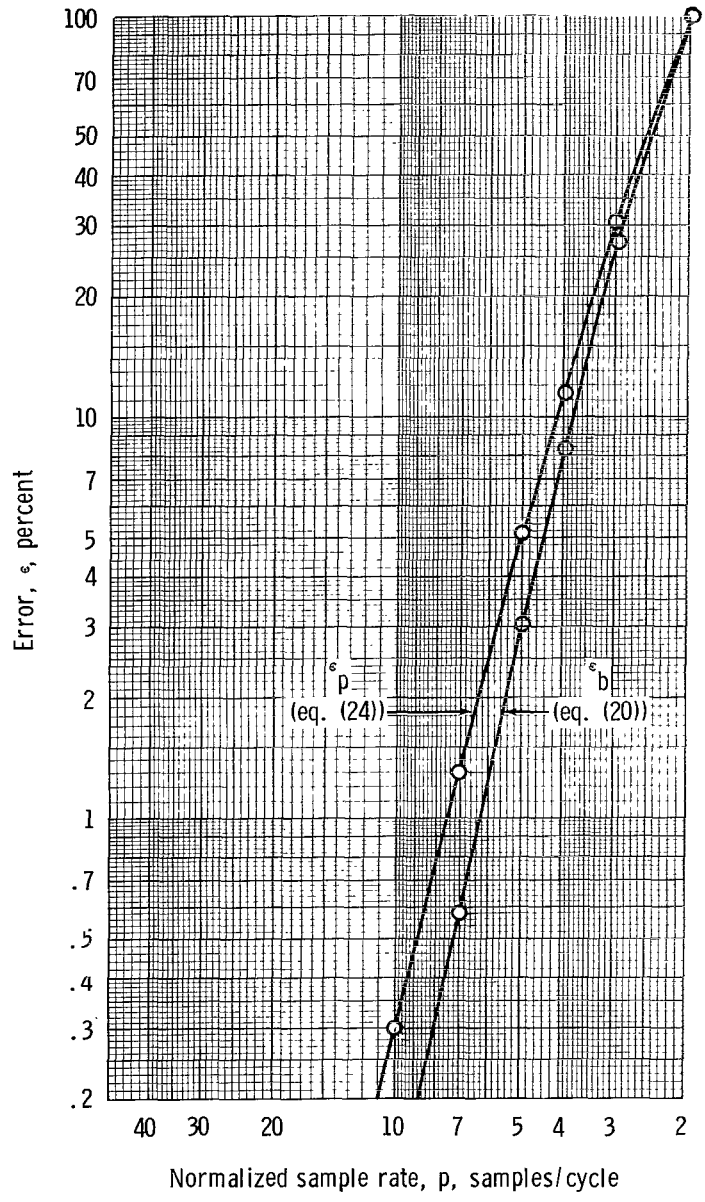

Figure 13. - Error as a function of normalized sample rate, third-order DAC.

EXPERIMENTAL RESULTS

As a means of checking the validity of the results of the preceding section, several variations of the data processing technique were simulated on a digital PCM system with a hybrid computer program. Conceptually, the system worked as indicated in figure 14. Table I is an explanation of the stages in figure 14 and in tables II and III.

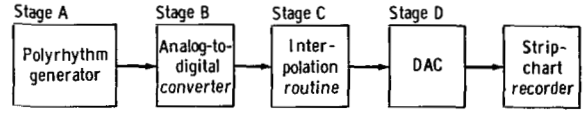

Figure 14. - Block diagram of the test system.

The experiment-control data processing technique was chosen to be the following: Stage A; stage B, items 1 and 3; stage C, item 1; and stage D. This variation is technique 08. The variations that are presented in the form of strip-chart recordings in figures 15 to 24 are given in table II. Each figure (figs. 15 to 24) shows the same set of data as it would appear after processing under the six variations listed in table II.

Tables IV to VIII are condensed summary listings of normal sinus data; the tables show peak values for the P-, Q-, R-, S-, and T-segments of the analog waveform on a cycle-to-cycle basis as the values would appear under the different processing techniques. Amplitude values are given in terms of PCM counts, ranging from 0 to 255. The data-processing-technique variations that were compared are shown in table III.

The analog data were artificially generated by a polyrhythm generator so that the waveform would remain stable from cycle to cycle. Hence, any variations in peak values of the output (the condensed summary listings) are caused by errors introduced by the different data processing techniques.

Figures 25 to 29 are graphic presentations of the results found in tables IV to VIII. These figures show the peak errors ϵ_p and the average peak errors, average ϵ_p, for the P-, Q-, R-, S-, and T-segments of the data as a function of the data processing technique. Also shown, in the interest of systems-engineering requirements, is the bandwidth (in bits/sec) required for transmitting the same set of data (three electrocardiograms) for each data processing technique.

The experimental results (figs. 25 to 29) confirm the analytical results (figs. 4 and 13). In performing a numerical comparison of the experimental results and the analytical results, the following factors must be considered:

1. Because of the digital nature of the system, the experimental data contain quantization noise, whereas the analytical results were derived for analog data without quantization noise.

2. Because of the analytical base (sinusoids), the error definition for the analytical results is in terms of percent of the maximum amplitude, whereas the experimental results, based on complex waveforms, required an error definition in terms of percent of full scale (255 PCM counts).

TABLE I. - DESCRIPTION OF TEST-SYSTEM STAGES AND CODES FOR STRIP-CHART RECORDINGS AND DIGITAL DATA

(a) Test-system stages

Stage	Description	Data
A	Several types of EKG analog data were used as input for the analog-to-digital converter.	1. Sinus bradycardia, 40 beats/min 2. Normal sinus, 80 beats/min 3. Sinus tachycardia, 120 beats/min 4. First-degree block at 80 beats/min 5. Second-degree block at 80 beats/min 6. Third-degree block at 80 beats/min 7. Atrial flutter 8. Atrial fibrillation 9. Ventricular tachycardia 10. Ventricular fibrillation
B	Various analog-to-digital converter variations were used.	1. 200 samples/sec 2. 100 samples/sec 3. Data quantized to 8 bits (256 levels) 4. Data quantized to 7 bits (128 levels) 5. Data quantized to 6 bits (64 levels)
C	Interpolation was performed by a digital computer.	1. If the input rate was 200 samples/sec, no interpolation was performed, and the output was 200 samples/sec (throughput). 2. If the input rate was 100 samples/sec, third-order interpolation was used to generate intermediate samples. a. For strip-chart recordings, an output rate of 200 samples/sec was used. b. For a check against the analytically predicted results, a summary listing of data points output at 1000 samples/sec was provided by the digital program.
D	The DAC was a standard zero-order DAC.	--

(b) Codes for strip-chart recordings and digital data

Code	Meaning	Description
O	Original data at 200 samples/sec	This was the control used in the experiment.
T	Truncated data	The number of possible levels used to describe an analog amplitude was reduced. This truncation was performed on an individual-sample basis.
C	Calculated data	The implication is that only 100 samples/sec of data were entered into the system and that these plus intermediate calculated samples, based on third-order polynomial computations, were output.
6, 7, and 8	--	These numbers indicate the number of bits used to represent the analog amplitude of each sample value.

TABLE II. - DATA-PROCESSING-TECHNIQUE VARIATIONS

FOR STRIP-CHART RECORDINGS

Technique	Components of the data processing technique
08	Stage A Stage B, items 1 and 3 Stage C, item 1 Stage D
T6	Stage A Stage B, items 1 and 5 Stage C, item 1 Stage D
C8	Stage A Stage B, items 2 and 3 Stage C, item 2a Stage D
C7	Stage A Stage B, items 2 and 4 Stage C, item 2a Stage D
[a]C7/T6	Stage A Stage B, items 2 and 4 Stage C, item 2a Stage D
C6	Stage A Stage B, items 2 and 5 Stage C, item 2a Stage D

[a]The T6 indicates that the output data were quantized to a 6-bit level after computation and before output.

TABLE III. - DATA-PROCESSING-TECHNIQUE VARIATIONS

FOR CONDENSED SUMMARY LISTINGS

Technique	Components of the data processing technique
08	Stage A, item 2 Stage B, items 1 and 3 Stage C, item 1
T6	Stage A, item 2 Stage B, items 1 and 5 Stage C, item 1
C8	Stage A, item 2 Stage B, items 2 and 3 Stage C, item 2b
C7	Stage A, item 2 Stage B, items 2 and 4 Stage C, item 2b
[a]C7/T6	Stage A, item 2 Stage B, items 2 and 4 Stage C, item 2b
C6	Stage A, item 2 Stage B, items 2 and 5 Stage C, item 2b

[a]The T6 indicates that the output data were quantized to a 6-bit level after computation and before output.

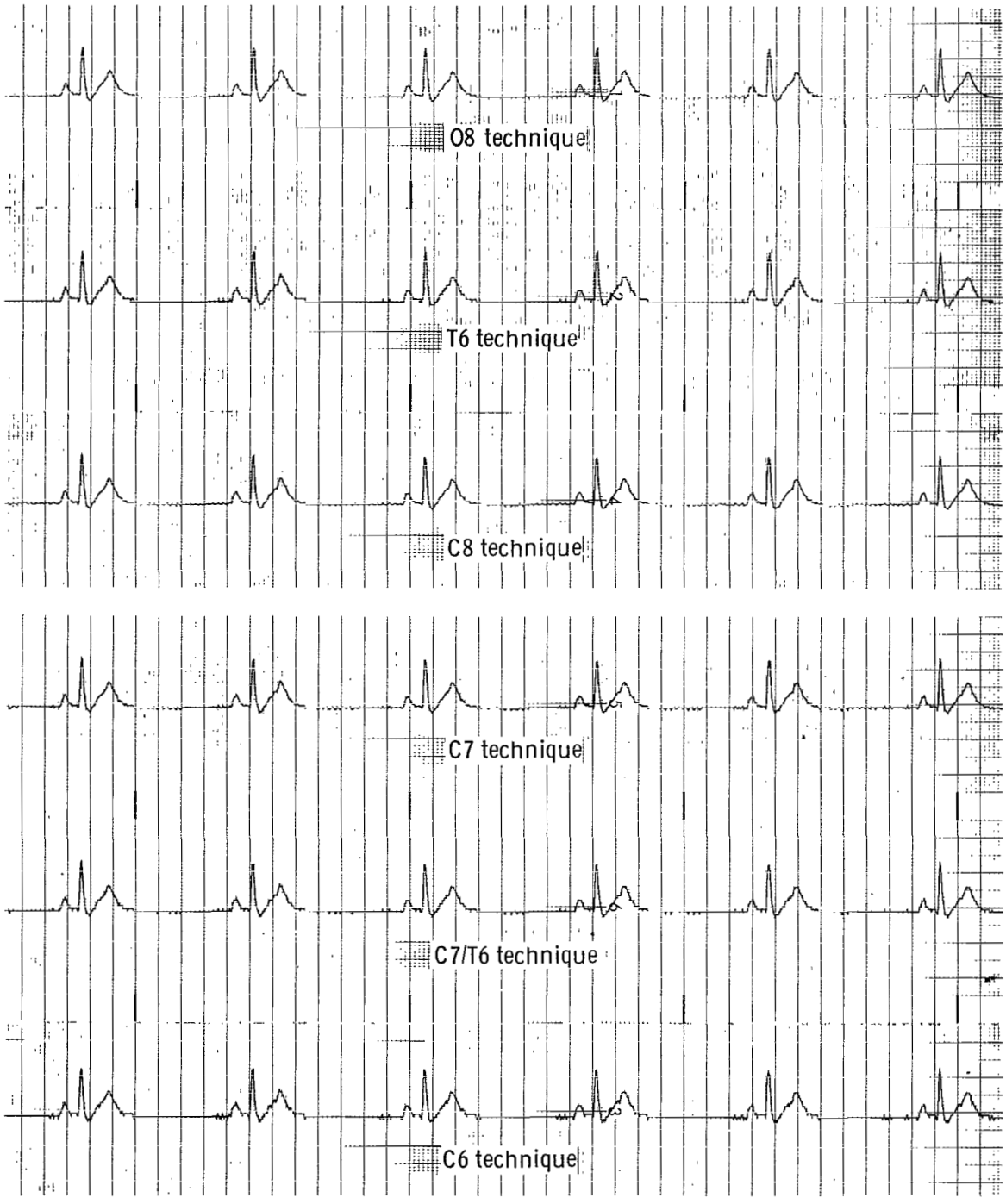

Figure 15. - Strip-chart recordings of sinus bradycardia, 40 beats/min.

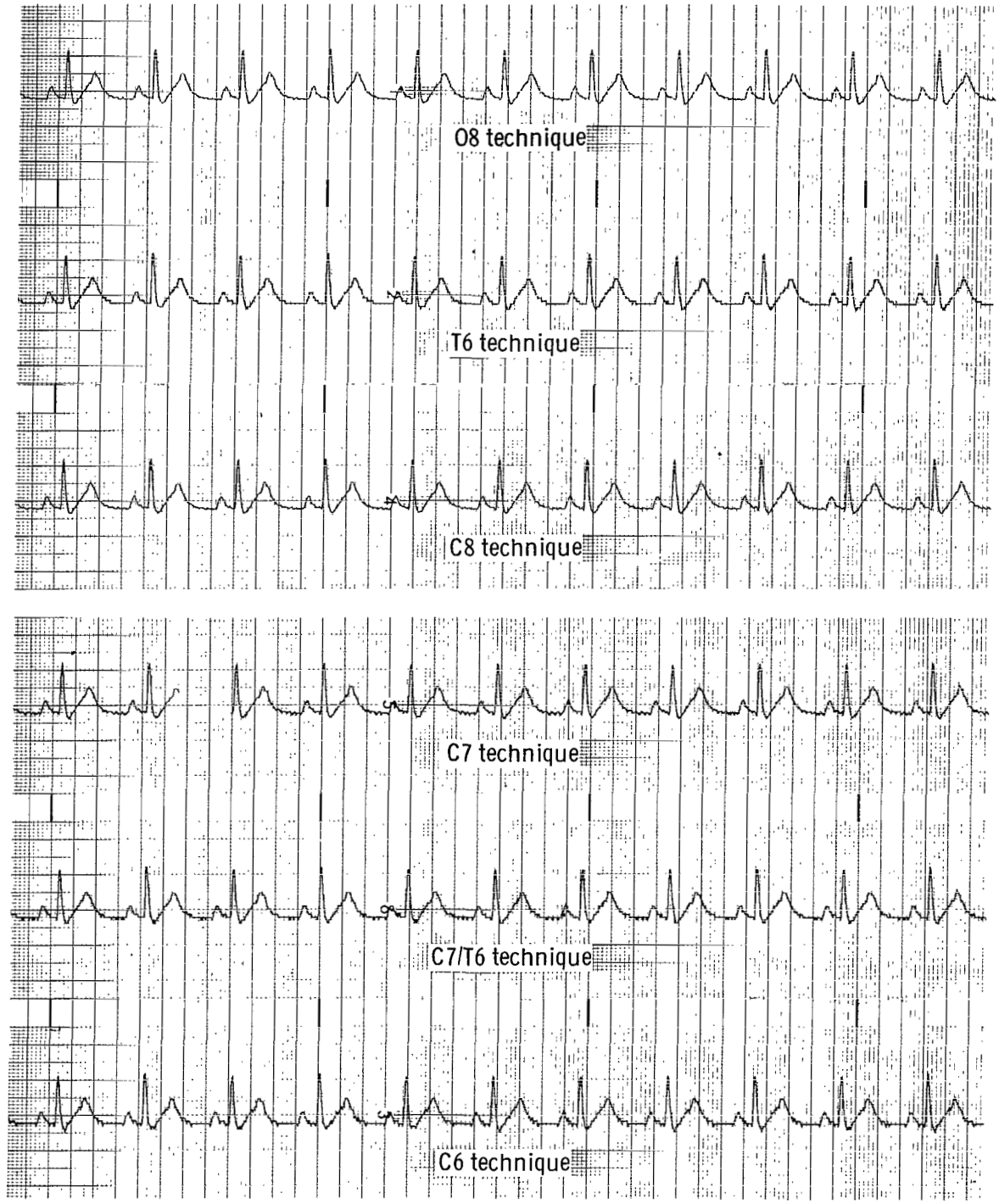

Figure 16. - Strip-chart recordings of normal sinus, 80 beats/min.

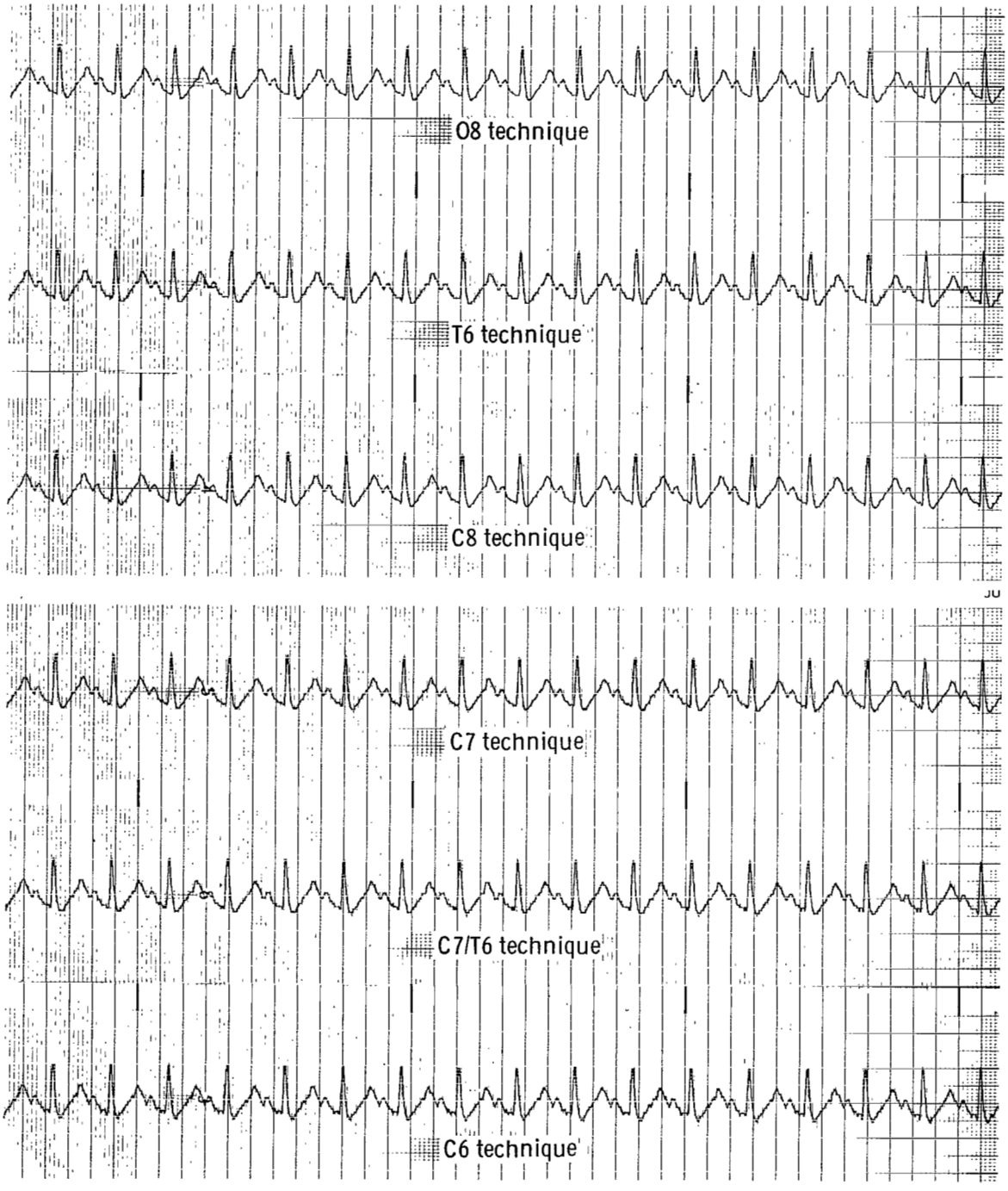

Figure 17. - Strip-chart recordings of sinus tachycardia, 120 beats/min.

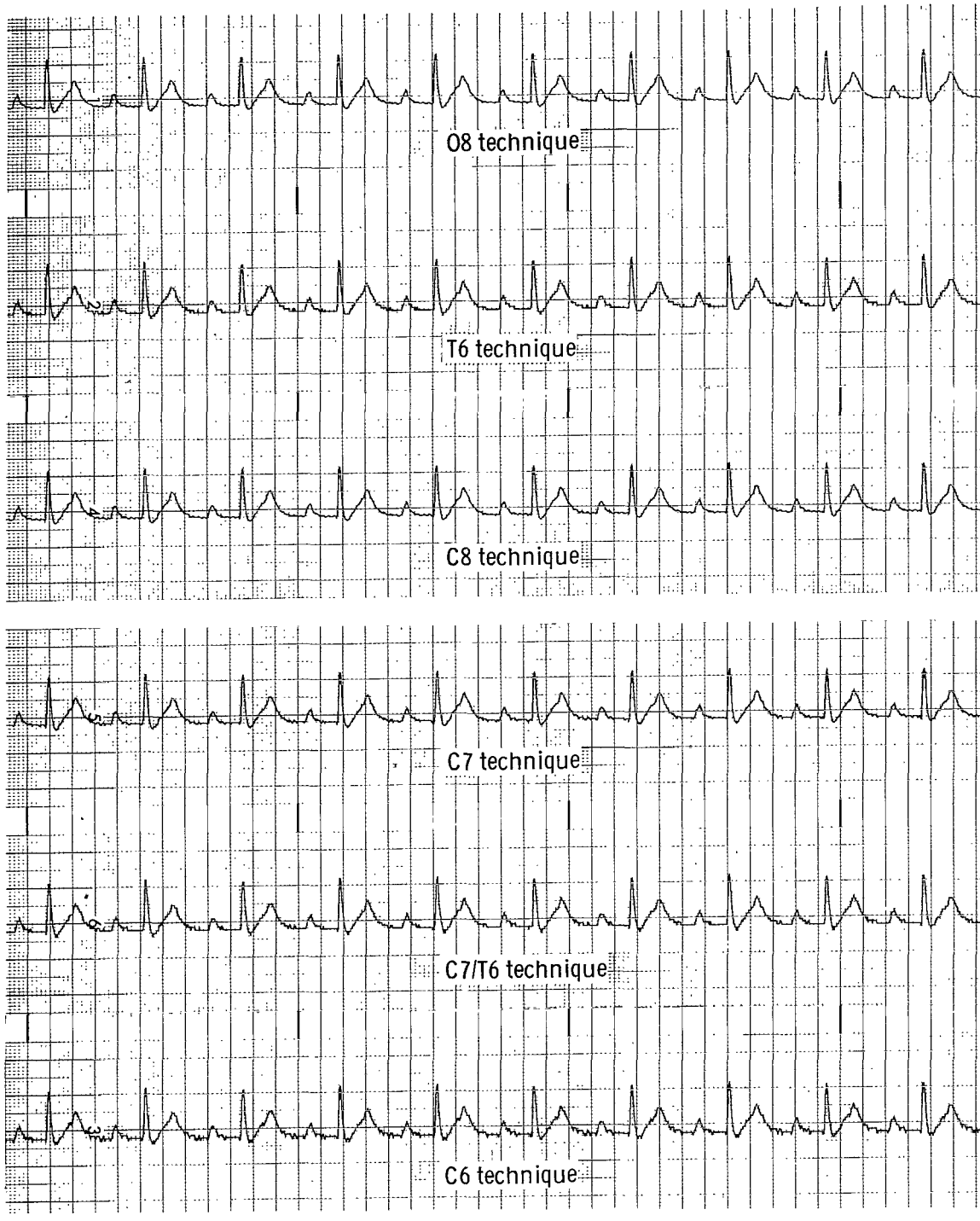

Figure 18. - Strip-chart recordings of a first-degree block, 80 beats/min.

Figure 19. - Strip-chart recordings of a second-degree block, 80 beats/min.

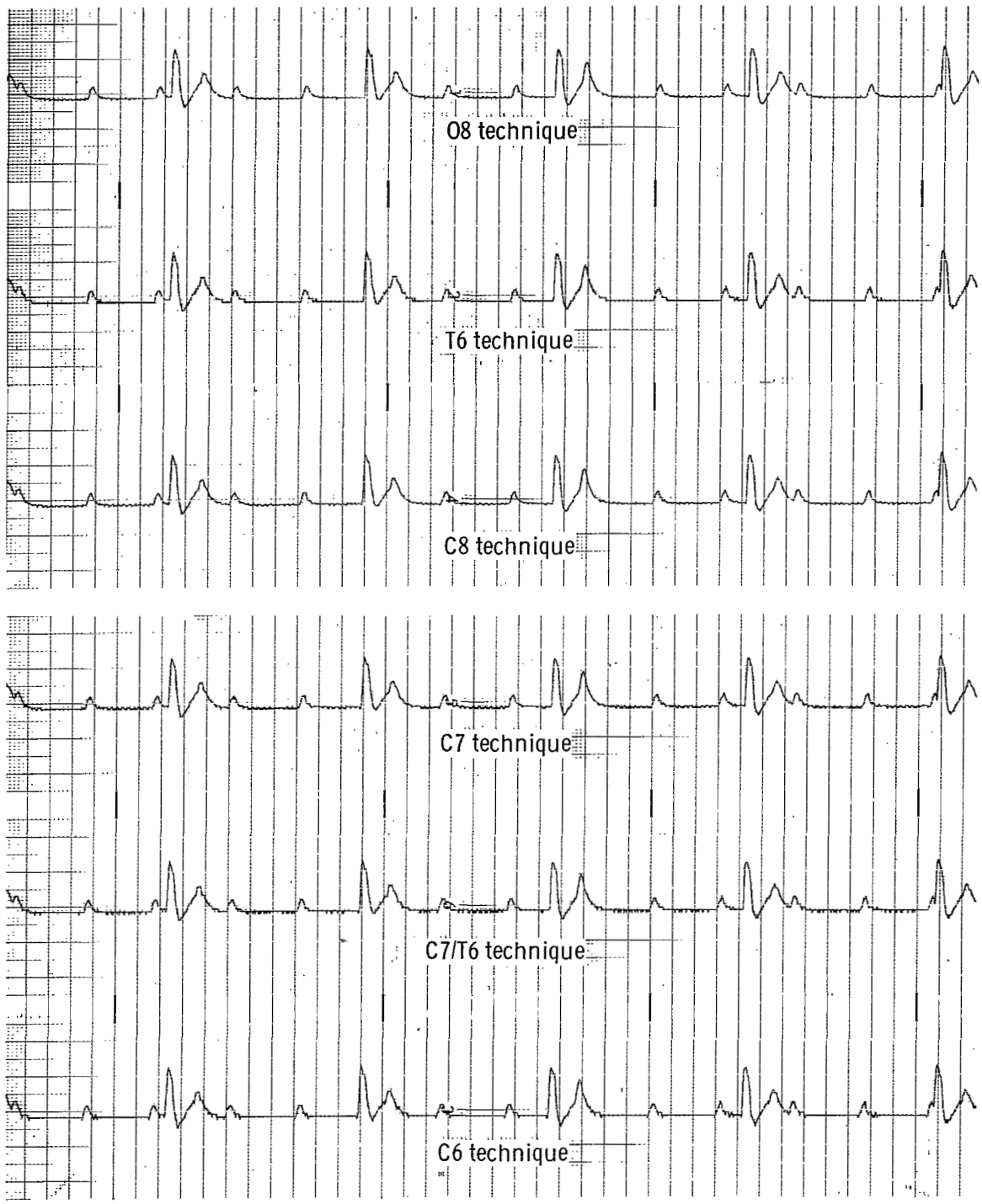

Figure 20. - Strip-chart recordings of a third-degree block, 80 beats/min.

Figure 21. - Strip-chart recordings of atrial flutter.

Figure 22. - Strip-chart recordings of atrial fibrillation.

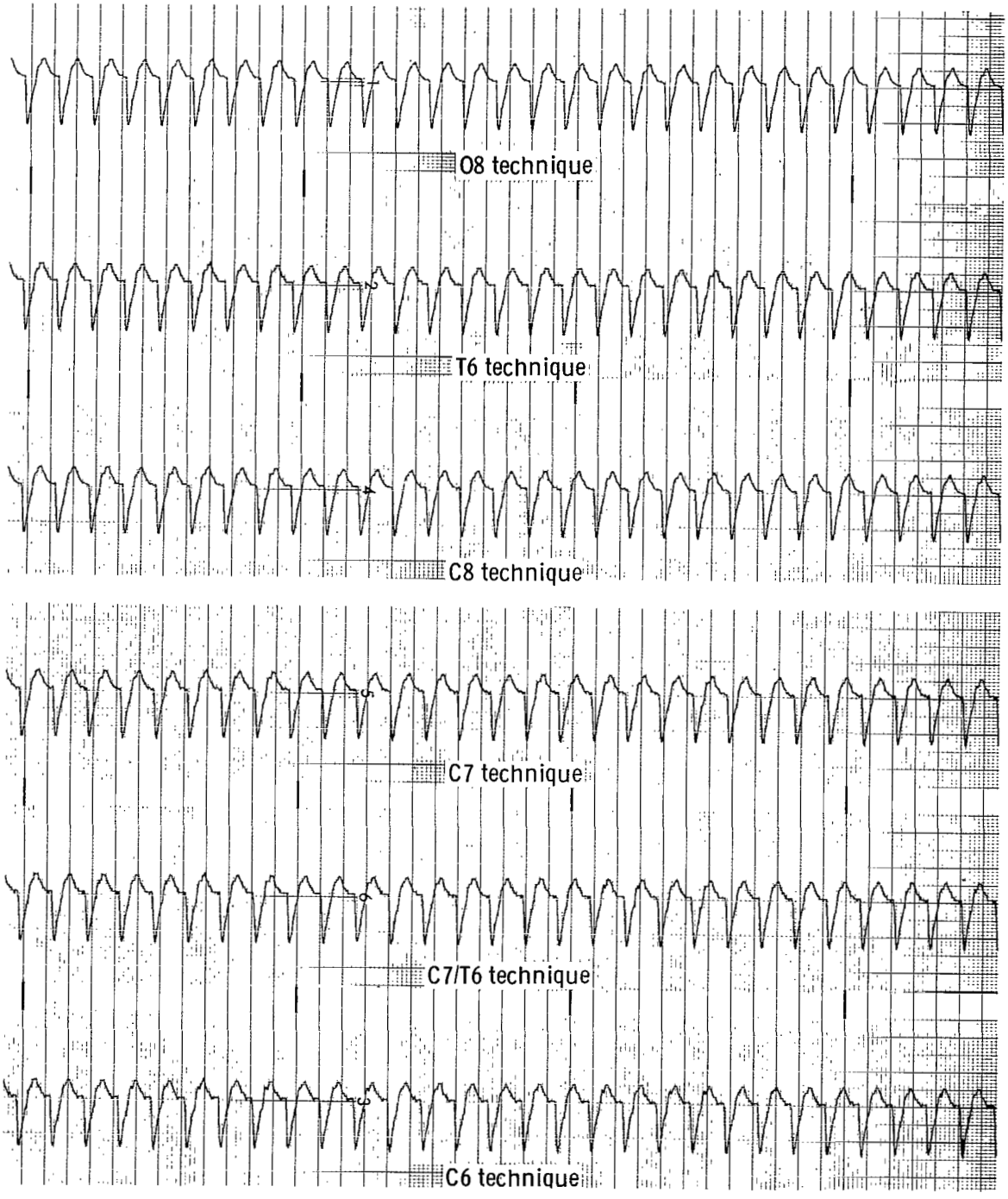

Figure 23. - Strip-chart recordings of ventricular tachycardia.

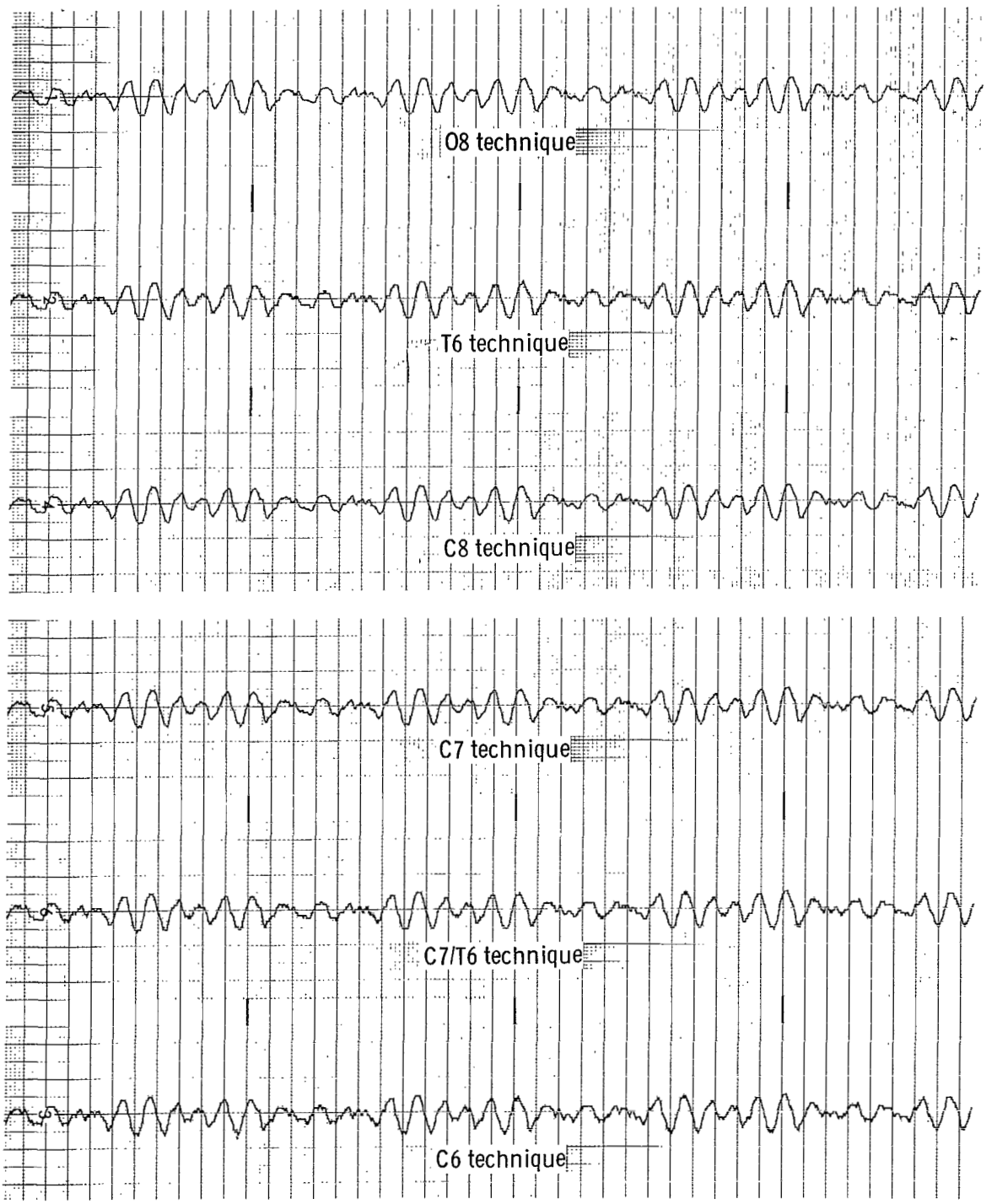

Figure 24. - Strip-chart recordings of ventricular fibrillation.

TABLE IV. - CONDENSED SUMMARY LISTING OF PEAK AMPLITUDES,

P-SEGMENT, NORMAL SINUS

Measurement	Peak amplitude, PCM counts, for data processing technique —					
	08	T6	C8	C7	C7/T6	C6
Cycle 1	135	132	135	134	132	132
Cycle 2	135	132	134	134	132	132
Cycle 3	135	132	135	134	132	132
Cycle 4	134	132	134	134	132	132
Cycle 5	135	132	135	134	132	132
Cycle 6	135	132	135	134	132	132
Cycle 7	135	132	135	134	132	132
Cycle 8	136	136	136	136	136	136
Cycle 9	134	132	134	134	132	132
Cycle 10	135	132	135	134	132	132
Average	134.9	132.4	134.8	134.2	132.4	132.4
Analog	136	136	136	136	136	136
Average ϵ_p	1.1	1.6	1.2	1.8	1.6	1.6
ϵ_p	2	4	2	2	4	4

TABLE V. - CONDENSED SUMMARY LISTING OF PEAK AMPLITUDES,

Q-SEGMENT, NORMAL SINUS

Measurement	Peak amplitude, PCM counts, for data processing technique —					
	08	T6	C8	C7	C7/T6	C6
Cycle 1	117	116	117	116	116	112
Cycle 2	117	116	116	114	112	112
Cycle 3	117	116	117	116	116	112
Cycle 4	117	116	116	114	112	112
Cycle 5	116	116	116	114	112	112
Cycle 6	117	116	117	116	116	112
Cycle 7	117	116	115	114	112	112
Cycle 8	117	116	115	114	112	112
Cycle 9	117	116	115	114	112	112
Cycle 10	116	116	114	112	112	112
Average	116.8	116.0	115.8	114.4	113.2	112.0
Analog	116	116	116	116	116	116
Average ϵ_p	.8	.0	.2	1.6	2.8	4.0
ϵ_p	1	0	2	4	4	4

TABLE VI. - CONDENSED SUMMARY LISTING OF PEAK AMPLITUDES,

R-SEGMENT, NORMAL SINUS

Measurement	Peak amplitude, PCM counts, for data processing technique —					
	08	T6	C8	C7	C7/T6	C6
Cycle 1	187	184	186	186	184	184
Cycle 2	187	184	187	186	184	184
Cycle 3	188	188	188	188	188	188
Cycle 4	187	184	187	186	184	184
Cycle 5	189	188	189	188	188	188
Cycle 6	187	184	187	186	184	184
Cycle 7	187	184	187	186	184	184
Cycle 8	188	188	187	186	184	184
Cycle 9	187	184	186	184	184	184
Cycle 10	189	188	187	186	184	184
Average	187.6	185.6	187.1	186.2	184.8	184.8
Analog	189	189	189	189	189	189
Average ϵ_p	1.4	3.4	1.9	2.8	4.2	4.2
ϵ_p	2	5	3	5	5	5

TABLE VII. - CONDENSED SUMMARY LISTING OF PEAK AMPLITUDES,

S-SEGMENT, NORMAL SINUS

Measurement	Peak amplitude, PCM counts, for data processing technique —					
	08	T6	C8	C7	C7/T6	C6
Cycle 1	111	108	111	110	108	108
Cycle 2	110	108	109	108	108	104
Cycle 3	112	112	111	110	108	108
Cycle 4	110	108	110	110	108	108
Cycle 5	111	108	110	110	108	108
Cycle 6	111	108	111	110	108	108
Cycle 7	110	108	110	108	108	104
Cycle 8	111	108	111	110	108	108
Cycle 9	110	108	109	108	108	104
Cycle 10	111	108	110	108	108	104
Average	110.7	108.4	110.2	109.2	108.0	106.4
Analog	110	110	110	110	110	110
Average ϵ_p	.7	1.6	.2	.8	2.0	3.6
ϵ_p	2	2	1	2	2	6

TABLE VIII. - CONDENSED SUMMARY LISTING OF PEAK AMPLITUDES, T-SEGMENT, NORMAL SINUS

Measurement	Peak amplitude, PCM counts, for data processing technique —					
	08	T6	C8	C7	C7/T6	C6
Cycle 1	154	152	154	154	152	152
Cycle 2	155	152	155	154	152	152
Cycle 3	154	152	154	154	152	152
Cycle 4	155	152	155	154	152	152
Cycle 5	155	152	155	154	152	152
Cycle 6	154	152	154	154	152	152
Cycle 7	155	152	155	154	152	152
Cycle 8	154	152	154	154	152	152
Cycle 9	155	152	155	154	152	152
Cycle 10	155	152	155	154	152	152
Average	154.6	152.0	154.6	154.0	152.0	152.0
Analog	155	155	155	155	155	155
Average ϵ_p	.4	3.0	.4	1.0	3.0	3.0
ϵ_p	1	3	1	1	3	3

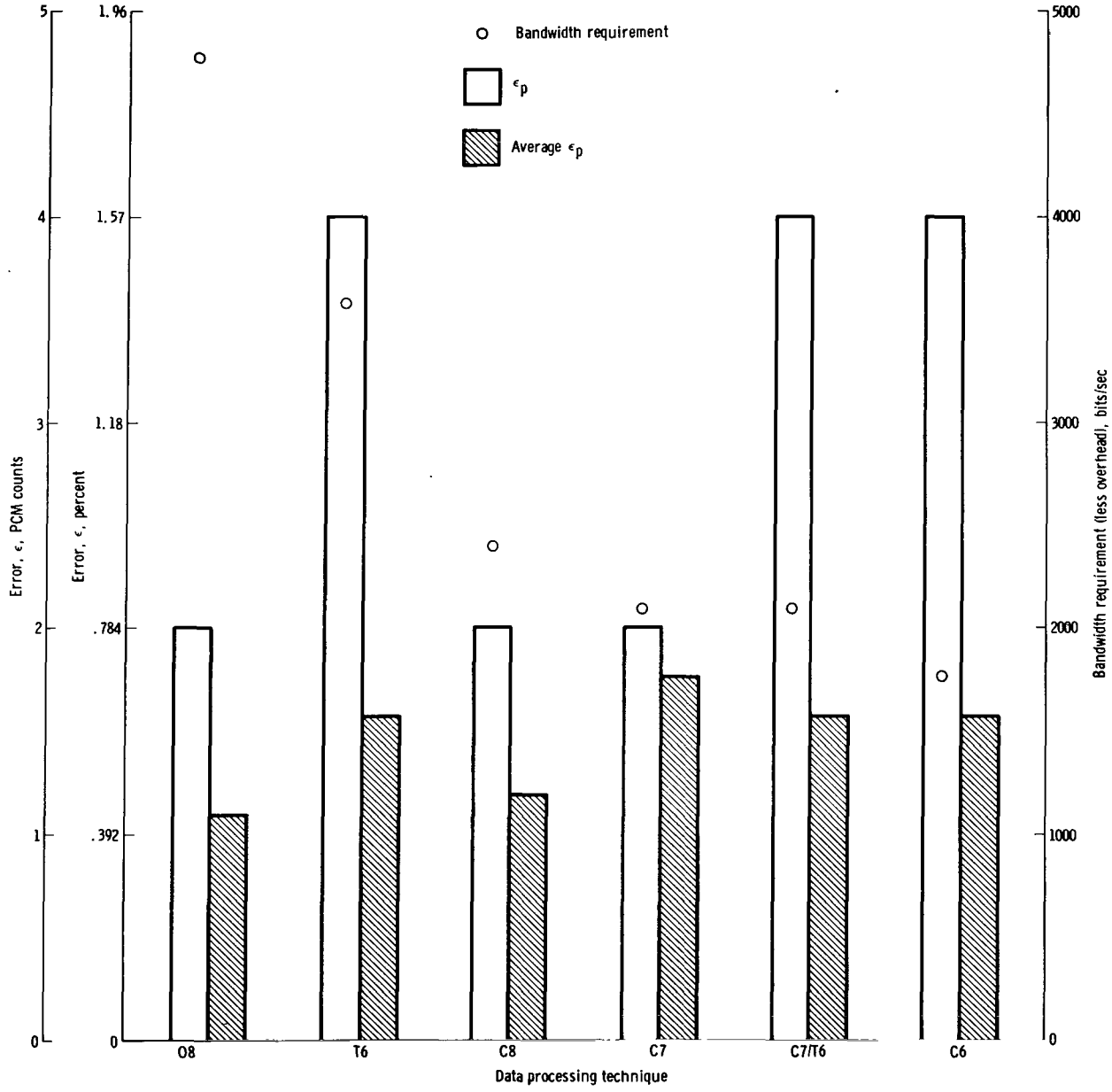

Figure 25. - Bandwidth requirement ϵ_p and average ϵ_p as functions of data processing technique for the P-segment of a normal sinus wave.

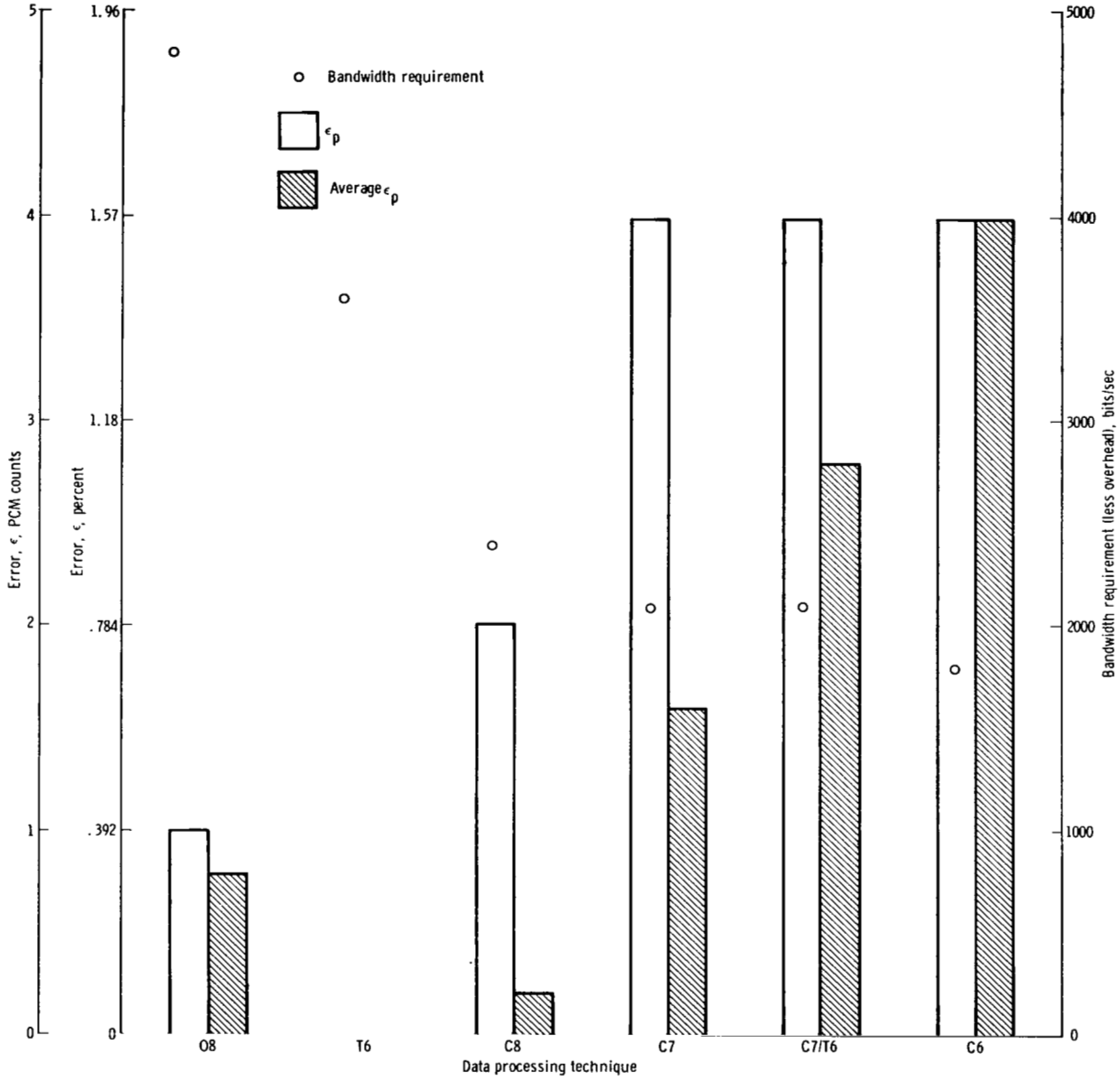

Figure 26. - Bandwidth requirement ϵ_p and average ϵ_p as functions of data processing technique for the Q-segment of a normal sinus wave.

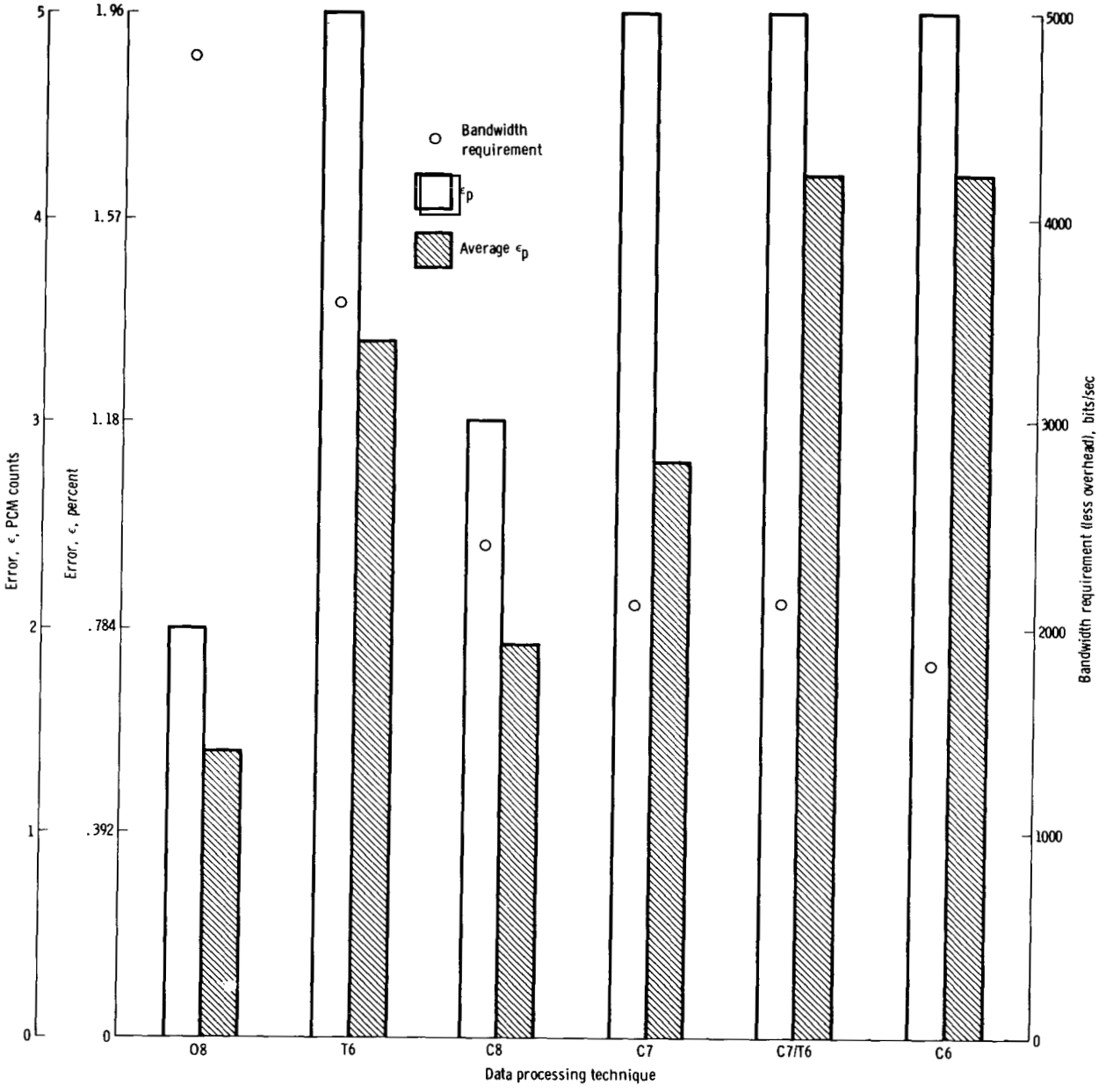

Figure 27. - Bandwidth requirement ϵ_p and average ϵ_p as functions of data processing technique for the R-segment of a normal sinus wave.

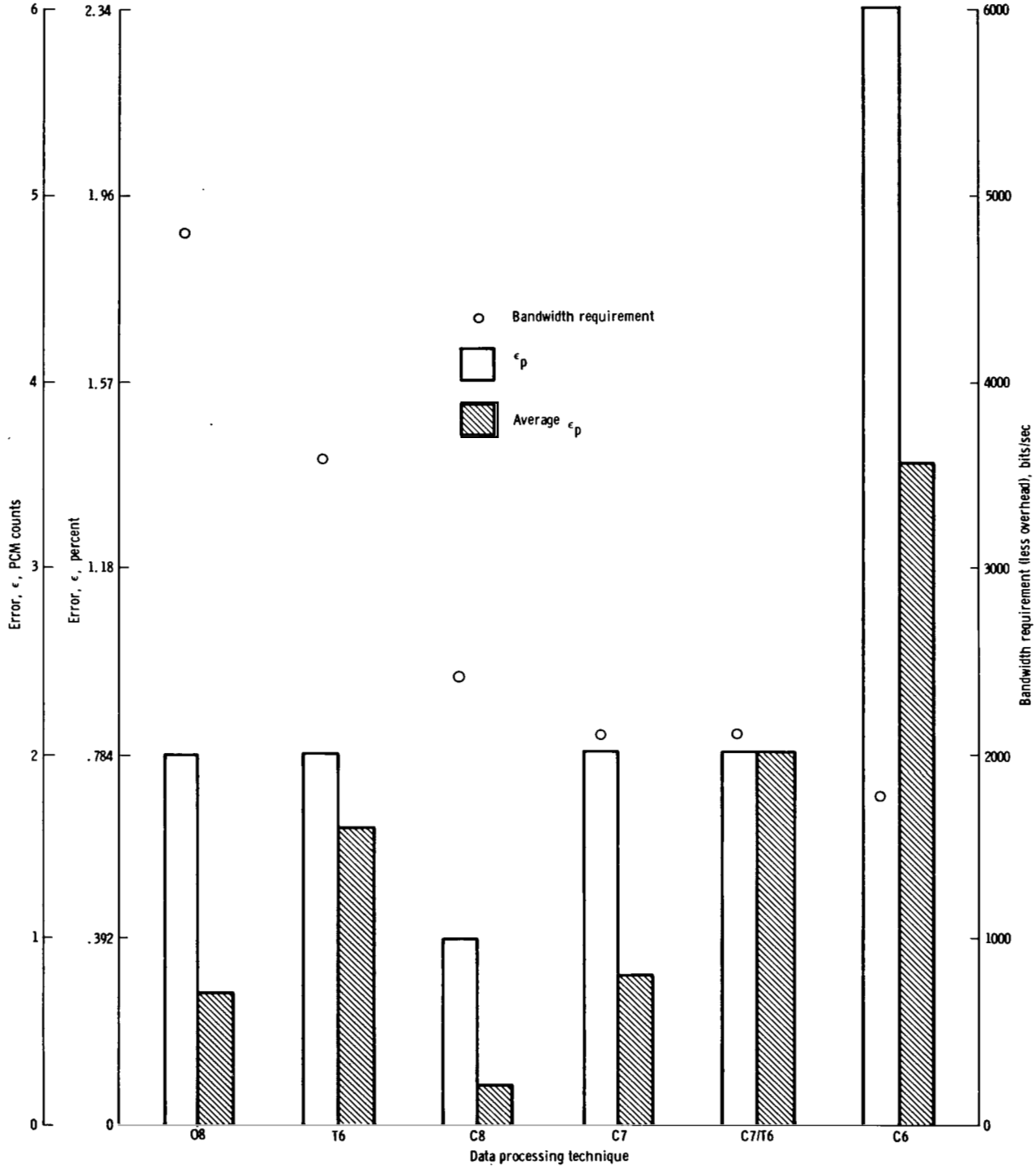

Figure 28.- Bandwidth requirement ϵ_p and average ϵ_p as functions of data processing technique for the S-segment of a normal sinus wave.

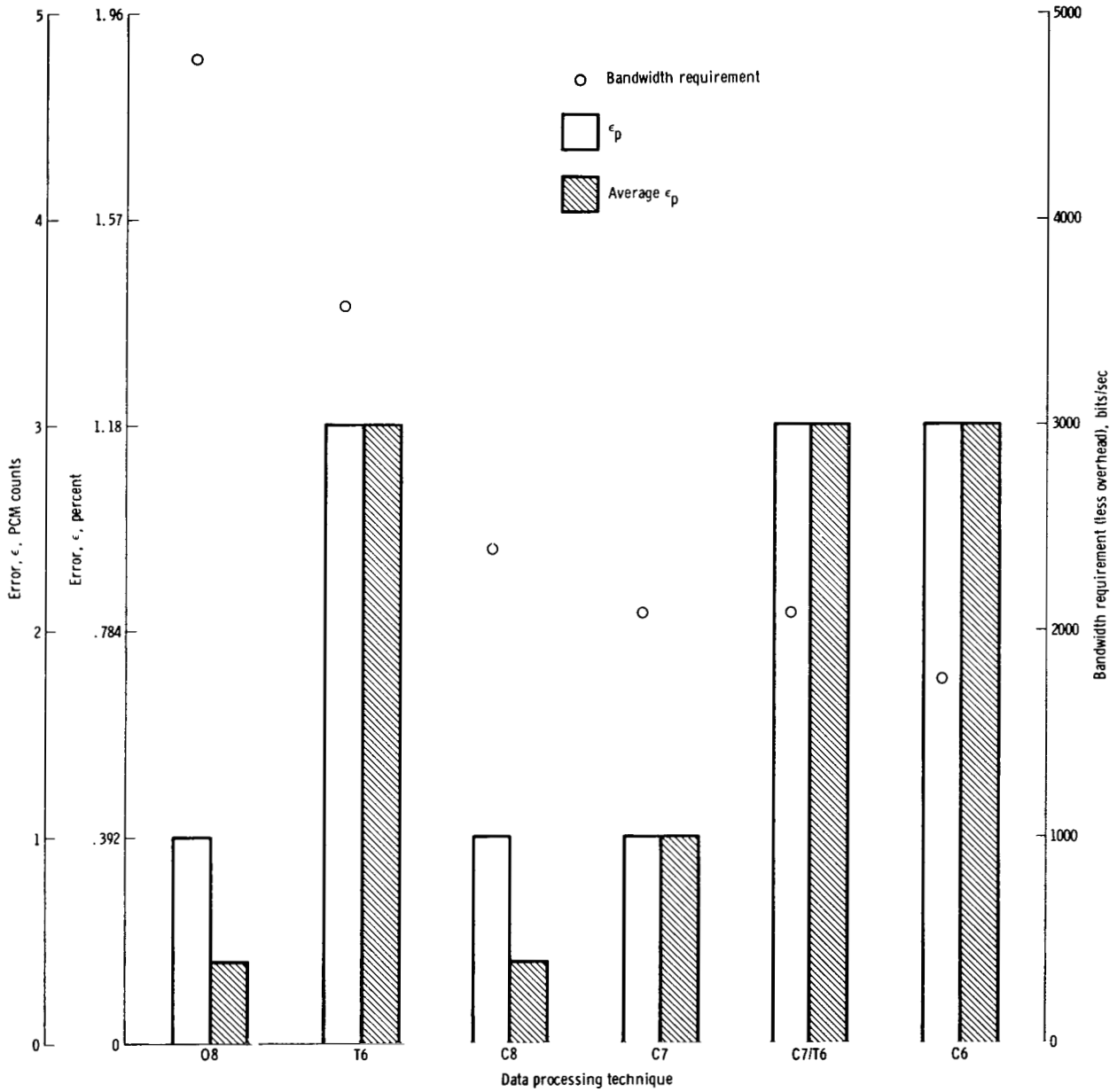

Figure 29. - Bandwidth requirement ϵ_p and average ϵ_p as functions of data processing technique for the T-segment of a normal sinus wave.

CONCLUSIONS

The data processing technique using calculated data quantized to an 8-bit level will provide (within the limits of quantization error) as accurate a reproduction of the electrocardiograms as the technique using the original data quantized to an 8-bit level; and the technique using the calculated 8-bit data will provide this reproduction with only half the bandwidth required by the technique using the original 8-bit data. Furthermore, the technique using the calculated 8-bit data is preferable, from both user and system viewpoints, to the technique using truncated data quantized to a 6-bit level, which is presently being implemented; that is, the technique using calculated 8-bit data is better in error performance, contains less quantization noise, and requires less bandwidth than the technique using truncated 6-bit data.

However, a problem exists in implementing the technique using calculated 8-bit data. The problem is a result of the system philosophy of designing only high-speed data-transfer formats containing whole-number multiples of 2400 bits. The technique using calculated 8-bit data requires precisely 2400 bits/sec for three electrocardiograms. Thus, because of this system philosophy, no allowances are made for impedance pneumograms or for overhead (both of which are necessary) in the same format.

The technique using calculated data quantized to the 7-bit level must then be considered. This technique is a solution to the problem mentioned in the previous paragraph and, from both user and system viewpoints, is also preferable to the technique using truncated 6-bit data. In an effort to reduce the required bit-rate bandwidth further, the techniques using calculated 7-bit data truncated to 6 bits and using calculated 6-bit data were tried. With these techniques, the error performance became slightly worse, but these techniques may be usable in the event of severe system constraints.

Finally, it should be noted that while the interpolation in this study was done by a digital computer, the interpolation could also be accomplished with a small, specialized analog computer. Such a device would generate, between the sample points, a piecewise continuous waveform which would effectively insert an infinite number of calculated points between the given sample points. Such an output would be more pleasing to the eye and would allow extremely accurate computation of segment durations of the electrocardiogram waveform, since the third-order digital-to-analog converter performance is even better near base-line crossings.

Manned Spacecraft Center
National Aeronautics and Space Administration
Houston, Texas, October 26, 1970
039-00-00-00-72

REFERENCE

1. Downing, John J.: Data Sampling and Pulse Amplitude Modulation. Chapter 4 of Aerospace Telemetry, Harry L. Stiltz, ed., Prentice-Hall, Inc. (Englewood Cliffs, N.J.), 1961, pp. 83-141.

"The aeronautical and space activities of the United States shall be conducted so as to contribute . . . to the expansion of human knowledge of phenomena in the atmosphere and space. The Administration shall provide for the widest practicable and appropriate dissemination of information concerning its activities and the results thereof."

— NATIONAL AERONAUTICS AND SPACE ACT OF 1958

NASA SCIENTIFIC AND TECHNICAL PUBLICATIONS

TECHNICAL REPORTS: Scientific and technical information considered important, complete, and a lasting contribution to existing knowledge.

TECHNICAL NOTES: Information less broad in scope but nevertheless of importance as a contribution to existing knowledge.

TECHNICAL MEMORANDUMS: Information receiving limited distribution because of preliminary data, security classification, or other reasons.

CONTRACTOR REPORTS: Scientific and technical information generated under a NASA contract or grant and considered an important contribution to existing knowledge.

TECHNICAL TRANSLATIONS: Information published in a foreign language considered to merit NASA distribution in English.

SPECIAL PUBLICATIONS: Information derived from or of value to NASA activities. Publications include conference proceedings, monographs, data compilations, handbooks, sourcebooks, and special bibliographies.

TECHNOLOGY UTILIZATION PUBLICATIONS: Information on technology used by NASA that may be of particular interest in commercial and other non-aerospace applications. Publications include Tech Briefs, Technology Utilization Reports and Technology Surveys.

Details on the availability of these publications may be obtained from:

SCIENTIFIC AND TECHNICAL INFORMATION OFFICE

NATIONAL AERONAUTICS AND SPACE ADMINISTRATION

Washington, D.C. 20546